LIMNOLOGY
and
OCEANOGRAPHY

ASLO

Limnol. Oceanogr. 62, 2017, 104–124

doi: 10.1002/lno.10379

Processes driving seasonal variability in DMS, DMSP, and DMSO concentrations and turnover in coastal Antarctic waters

E. C. Asher,[1,a]* J. W. H. Dacey,[2] M. Stukel,[3] M. C. Long,[4] P. D. Tortell[1,5]

[1]Earth, Ocean and Atmospheric Sciences, University of British Columbia, Vancouver, British Columbia, Canada
[2]Department of Biology, Woods Hole Oceanographic Institution, Woods Hole, Massachusetts
[3]Department of Earth, Ocean and Atmospheric Science Florida State University, Tallahassee, Florida
[4]Climate and Global Dynamics, National Center for Atmospheric Research, Boulder, Colorado
[5]Department of Botany, University of British Columbia, Vancouver, British Columbia, Canada

Abstract

This study presents new measurements of the concentrations and turnover rates of dimethyl sulfide (DMS), dimethylsulfoniopropionate (DMSP), and dimethyl sulfoxide (DMSO) in coastal waters near Palmer Station, Antarctica, during the spring and summer of 2012–2013. Using several novel analytical and experimental techniques, we document variability in DMS, DMSP, and DMSO (DMS/P/O) concentrations and quantify dominant production and removal terms in the mixed layer DMS budget. Our results demonstrate considerable seasonal variability in the concentration of DMS (range 0–20 nM), total DMSP (8–160 nM), and total DMSO (4–160 nM). Over the seasonal cycle, dissolved DMSP concentrations were well correlated with total DMSP concentrations and the abundance of *Phaeocystis antarctica*, while DMSO concentrations (total and dissolved) were well correlated with DMS concentrations. DMSP cleavage from the dissolved pool (mean rate = 5.5 nM d^{-1}) and release from microzooplankton grazing (mean 5.6 nM d^{-1}) were the dominant sources of DMS, with smaller DMS production rates associated with DMSO reduction from the dissolved pool (mean 2.6 nM d^{-1}) and krill grazing (mean 0.82 nM d^{-1}). Specific rate constants for DMSP cleavage were inversely related to net primary production. Bacterial uptake was a primary contributor to DMS removal (mean −12 nM d^{-1}), and we observed a significant correlation between bacterial production and gross DMS loss rate constants. Estimated sea-air flux and photo-oxidation constituted secondary DMS sinks. Our experimental and analytical methods provide insight into the DMS/P/O cycle at Palmer Station, and a starting point for future studies examining inter-annual DMS/P/O variability in coastal Antarctic waters.

The trace gas dimethyl sulfide (DMS) is the main source of natural, non-sea-salt sulfate to the atmosphere (Bates et al. 1992; Gondwe et al. 2003), a key player in the global sulfur cycle and atmospheric radiative balance (Lovelock et al.1972; Charlson et al. 1987; Mahajan et al. 2015), and an important compound for the metabolism of several marine trophic groups. The gas is largely derived from the algal metabolite dimethylsulfoniopropionate (DMSP), which serves a number of physiological functions, including potential roles as an osmolyte (Dickson and Kirst 1987), cryoprotectant (Kirst et al. 1991), and anti-oxidant (Sunda et al. 2002). Particulate DMSP ($DMSP_p$) in phytoplankton is released into the dissolved pool ($DMSP_d$) through phytoplankton mortality and exudation (Laroche et al. 1999), and actively taken up by microorganisms (Kiene and Linn 2000; Vila-Costa et al. 2006a, 2008; Spielmeyer et al. 2011) and higher trophic levels (Levasseur et al. 1994; Kwint and Kramer 1996; Curson et al. 2009). The uptake and assimilation of $DMSP_d$ can satisfy the energy, carbon and sulfur demands of entire marine bacterial communities (Kiene and Linn 2000), and this compound also serves as a chemoattractant for a wide array of microorganisms (Seymour et al. 2010). By comparison with DMS and DMSP, the physiological and ecological function of dimethylsulfoxide (DMSO) remains less well studied. This compound is a main product of biological and photochemical DMS oxidation, and is ubiquitous in surface ocean waters. It has been suggested to function as an

*Correspondence: elizabethcolleenasher@gmail.com

[a]Present address: Department of Land Air and Water Resources, University of California, Davis

Additional Supporting Information may be found in the online version of this article.

intracellular cryoprotectant and anti-oxidant (Hatton et al. 2005).

A primary focus of DMS, DMSP, and DMSO (DMS/P/O) research is to understand the spatial and temporal variability of these compounds in oceanic waters, and quantify the underlying production and consumption processes. Rapid biological production and consumption of DMS/P/O has been documented in many marine environments, yielding short (i.e., < 1–5 d) turnover times, and significant small-scale spatial and temporal variability in concentrations. In the surface ocean, DMS is produced through the cleavage of $DMSP_d$ by phytoplankton and bacteria (Kiene and Linn 2000; Luce et al. 2011), and the intra-cellular cleavage of phytoplankton particulate DMSP ($DMSP_p$) catalyzed by the enzyme DMSP lyase. DMS may also be produced through the photochemical and biological reduction of DMSO to DMS (Fuse et al. 1995; Spiese et al. 2009; Asher et al. 2011), or released to the water column during zooplankton grazing (Dacey and Wakeham 1986; Archer et al. 2001, 2003; Salo et al. 2010). The removal of DMS and DMSP occurs via bacterial consumption (Wolfe et al. 1999; Vila-Costa et al. 2006b; Del Valle et al. 2007, 2009) and, in the case of DMS, sea-air flux and photochemical oxidation to DMSO or other products such as sulfate or dimethyl sulfone (Kieber et al. 1996; Del Valle 2009). In addition, dilution of these compounds in the surface ocean occurs through lateral advection and vertical mixing (Le Clainche et al. 2006).

Whereas many of the physical processes influencing DMS/P/O concentrations in seawater can be quantified from environmental variables (e.g., density gradients, wind speeds, and surface irradiance) and well represented in ocean models, biological cycling processes have proven difficult to quantify directly and to parameterize mechanistically. Over the past decade, however, the development of new experimental approaches has improved the quantification of several biological production/consumption processes in the oceanic DMS/P/O cycle. For instance, rates of DMSP synthesis have been quantified through the incorporation of 13C into DMSP (Stefels et al. 2009), and radioactively labeled DMS/P has proven to be an invaluable tool for quantifying DMS/P biological consumption rates and production yields (i.e., net DMS yield from DMSP-consumption; Kiene and Linn 2000; Zubkov et al. 2002; Toole et al. 2004; Merzouk et al. 2006; Vila-Costa et al. 2006b; Del Valle et al. 2007, 2009; Lizotte et al. 2009; Luce et al. 2011). More recently, a new stable isotope tracer method has been developed to simultaneously track the production and consumption of various compounds in the sulfur cycle, and this method has revealed rapid turnover of DMS/P/O in Antarctic sea-ice (Asher et al. 2011). To date, these new experimental approaches have only been applied in a handful of oceanic environments.

The Southern Ocean contains the world's highest marine surface water DMS concentrations and contributes significantly to global oceanic DMS sea-air flux (Lana et al. 2011; Jarníková and Tortell 2016). Strong seasonal cycles in sea-ice cover, solar irradiance, wind-speed, and mixed layer depth result in highly dynamic biological production (Arrigo et al. 2008), which drives strong variability in surface DMS/P/O concentrations (DiTullio et al. 2000; Kiene et al. 2007; Tortell and Long 2009; Tortell et al. 2011). Disentangling spatial gradients from temporal variability in such dynamic systems is challenging using ship-based surveys at discrete hydrographic sampling stations. To address this problem, several Lagrangian studies have been conducted in the Southern Ocean (Boyd et al. 2000; Wingenter et al. 2004; Yang et al. 2013), tracking individual water masses to isolate temporal variability from the underlying spatial heterogeneity. These studies have demonstrated a strong (often dominant) imprint of biological production and consumption on DMS cycling, and have examined the response of DMS and DMSP concentrations to large-scale Fe manipulations.

A deeper understanding of the seasonal dynamics of Southern Ocean DMS requires observations on time-scales that are beyond the scope of ship-based programs. Fortunately, there are several well-equipped Antarctic research stations with access to coastal seawater. The Palmer Station Long Term Ecological Research Site (PAL-LTER) is located on the northwest coast of the Antarctic Peninsula. For over two decades, the PAL-LTER program has documented the seasonal and interannual variability of microbial populations and productivity (http://pal.lternet.edu), demonstrating strong changes in microbial processes both within and between years, as well as long-term ecological changes along the Western Antarctic Peninsula (WAP) associated with rapid regional warming (Stammerjohn et al. 2008). The extent to which these shifts in the marine food web influence the biogeochemical cycling of trace gasses such as DMS has not been extensively studied.

Thus far, two dedicated DMS research programs have been conducted at Palmer Station. Berresheim et al. (1998) focused on quantifying the seasonal cycle of atmospheric DMS concentrations, and reported a close relationship between atmospheric and sea surface DMS levels. In a subsequent study, a group of international investigators examined the seasonal and depth-dependent variability in DMS concentrations and loss pathways for DMS/P during austral spring and summer at two stations on the Palmer Station LTER grid. Results from this field program (Hermann et al. 2012) showed that DMS concentrations tracked phytoplankton biomass, exhibited considerable seasonal variability and reached values as high as ~20 nM. During the study period, microbial consumption dominated DMS removal, with smaller DMS losses attributed to photochemical oxidation, sea-air flux, vertical mixing and entrainment. Based on an analysis using a one-dimensional ocean model, combined with semi-weekly in situ DMS concentration and consumption measurements, Hermann et al. (2012) derived an average gross DMS production rate of 3.1 ± 0.6 nM d^{-1}. This work provided important new insight into the seasonal

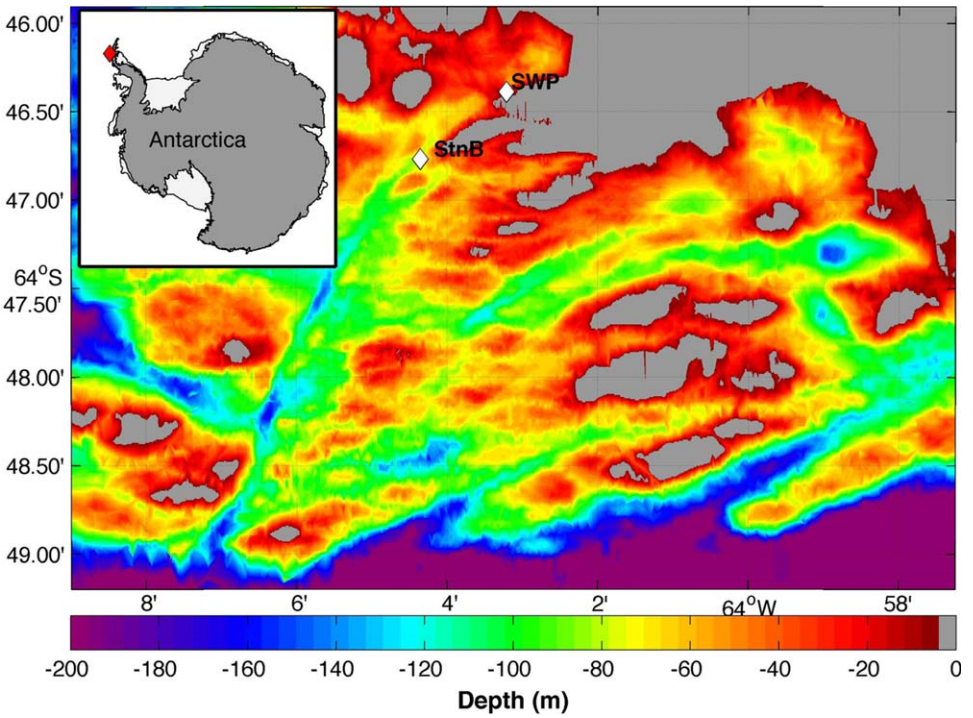

Fig. 1. A map of the study area, showing bathymetry (on color scale) and the location of the seawater pump intake (SWP) from which seawater was continuously sampled, and station B (Stn B), where discrete bottle samples were obtained.

dynamics of DMS in coastal WAP waters, but it did not assess the relative importance of various processes driving the biological production of DMS (e.g., grazing, $DMSP_d$ cleavage, $DMSO_d$ reduction), or the decoupling of DMS production and loss rate constants.

Building on the studies discussed above, we present new results from a recent field program at Palmer Station, aimed at documenting temporal variability in surface seawater DMS/P/O concentrations and turnover rates during the spring and summer phytoplankton growth season. We collected samples for DMS/P/O analysis in conjunction with the semi-weekly Palmer-LTER sampling program, and made additional high temporal resolution measurements of DMS. To quantify the production and consumption of DMS through various biotic and abiotic pathways, we used gross DMS production assays with competitive inhibitors, and recently developed stable isotope tracer assays (Asher et al. 2011). We also conducted experiments to examine the influence of microzooplankton and krill grazing on DMS production. We use our results to document short-term and seasonal patterns in DMS/P/O cycling in coastal Antarctic waters, and to suggest priorities for future studies.

Methods

Sampling overview

We conducted a field campaign between October 2012 and March 2013 at Palmer Station. Discrete semi-weekly samples were collected from Station B of the LTER sampling grid (64.78 S 64.07 W), which is situated off of Bonaparte Point adjacent to a deep trough (Fig. 1). The discrete samples were collected to measure the seasonal evolution of DMS/P/O concentrations in coastal WAP waters, and to conduct process studies examining the underlying production and consumption rates through various pathways. The semi-weekly concentration samples were supplemented with continuous automated analysis of DMS from the station's unfiltered seawater pump supply (SWP) located in Arthur Harbor (Fig. 1). Discrete DMS/P/O samples were analyzed using a sulfur chemiluminescence detector (SCD), while continuous DMS measurements were made by membrane inlet mass spectrometry (MIMS; Tortell 2005). The analytical methods for these sulfur concentration measurements and the ancillary measurements are described in detail in the Supporting Information. Below, we describe our sampling methodology, data processing and analysis of novel stable isotope and grazing rate measurements.

Process studies and rate experiments

A variety of experimental studies were conducted to quantify rates of key DMS/P/O production and consumption processes over the seasonal cycle. For all rate experiments, seawater was collected from station B (see Fig. 1) into a 10% HCl rinsed 20 L carboy. We conducted four types of rate

Table 1. Equations for the derivation of various rates described in the methods. In these equations, k is a rate constant (d^{-1}), t is for time, the subscript t is for an individual time-point measurement, the subscript 0 is for the initial measurement at T_0, and the subscript *corr* denotes a signal corrected for background interferences.

1. $natural\ DMS = m62\ DMS - 0.01 * m68\ DMS$
2. $\ln \frac{[DMS_{unlabeled}]_t}{[DMS_{unlabeled}]_0} = k_{dms\_production} t$
3. $\ln \frac{[DMSP_{unlabeled}]_t}{[DMSP_{unlabeled}]_0} = k_{dmsp\_production} t$
4. $\ln \frac{[D-3\ DMS]_t}{[D-3\ DMS]_0} = -k_{dms\_cons} t$
5. $[C13_2DMS] = [DMS_{64}] - 0.3\ [DMS_{65}] - 0.043\ [DMS_{62}]$
6. $[C13_2DMS]_{corr} = [C13_2DMS] + \frac{[C13_2DMS]_0}{e^{-k_{DMS\_cons} t}}$
7. $In \frac{[C13_2 - DMS]_{t\ corr}}{[C13_2 - DMS]_{0\ corr}} = K_{DMSO\_reduction} t$
8. $[D-6\ DMS]_{corr} = [D-6\ DMS] + \frac{[D-6\ DMS]_0}{e^{-k_{DMS\_cons} t}}$
9. 6. $In \frac{[D-6\ DMS]_{t\ corr}}{[D-6\ DMS_0]} = K_{\_cleav} t$
10. $DMS_{microzoo\_prod} = DMS_{prod\_fract} * DMSP_{p\_graz} * [DMSP_p]$
11. $DMS_{krill\_prod\ WAP} = DMS_{nM\ d^{-1}} * Krill_{ind\ m^{-2}} * \frac{1m^3\ X\ 50L}{1000\ L\ X\ Depth\ (m)\ X\ Krill\ (ind)}$
12. $\text{Net DMS Prod} = DMS_{microzoo\_prod} + DMS_{krill\_prod\ WAP} + DMS_{DMSP\_Cleav} + DMS_{DMSO\_Red} - DMS_{gross\_cons} - DMS_{flux}$

experiments: (1) gross DMS production (GP) experiments, (2) stable-isotope tracer experiments, (3) dilution microzooplankton grazing experiments, and (4) krill grazing experiments.

Competitive inhibitor (CI) gross DMS production experiments

In gross production experiments, we measured the net change in DMS or DMSP concentrations in the presence of competitive inhibitors blocking the uptake of these compounds. For gross DMS production experiments, we used stable isotope labeled D-6 DMS (CDN isotopes D-1509) to inhibit the consumption of DMS. D-6 DMS has all six hydrogen atoms on the two CH_3 groups replaced with dueterium, and we have found that kinetic isotope effects, based on discrimination against D-6 DMS over naturally occurring DMS, are too small to detect using PT-CIMS (Asher et al. unpubl. data). The deuterium-labeled DMS can thus be used as a competitive analog of naturally occurring DMS, blocking uptake of unlabeled DMS. In our experiments, we used additions 1.5 μM D-6 DMS to competitively inhibit DMS uptake, such that measured changes in DMS concentrations reflected gross DMS production. To quantify gross DMSP production rates, we used 1.7 μM Glycine Betaine to competively block $DMSP_d$ uptake (Kiene and Gerard 1995). Natural seawater samples without any inhibitor additions were used as control replicates for these experiments, in which net changes in DMS and DMSP were measured.

After adding competitive inhibitors of DMS or DMSP uptake to samples, incubation bags were mixed by inverting 10 times. Subsamples were collected using a 60 mL luerlok BD syringe through a Teflon bag port equipped with luerlok fittings. The UV transparent bags were immediately transferred to an outdoor incubator maintained close to ambient sea surface temperature by a continuous flow of surface seawater. The bags were covered with one or two layers of neutral density coarse mesh screening, which reduced light levels to ~50% of sea surface values, without influencing the spectral quality of irradiance (neutral density screening is transparent to all wavelengths, including UV and uniformly reduces the light intensity across all wavelengths). Over the course of ~6 h, subsamples were filtered every ~1.5 h through an acrodisc GF/F filters (nominal pore size ~0.7 μm) into a 50 mL pre-cleaned (soaked in 10% HCl) glass serum bottles. Filtered samples were analyzed, as described below, using a purge and trap capillary inlet mass spectrometer (PT-CIMS).

The purge and trap capillary inlet mass spectrometry (PT-CIMS) used in this study has been described by Asher et al. (2011). Briefly, this analytical system couples a custom-built purge and trap gas extraction system with gas chromatographic separation of various sulfur compounds and detection using Hiden Analytical quadrupole mass spectrometer.

Our PT-CIMS has a detection limit of ~0.1 nM DMS in 50 mL samples, and enables us to discriminate the isotopically labeled D-6 DMS competitive inhibitor (m/z 68) from natural (unlabeled) DMS (m/z 62). In our experiments, we used 50 mL subsamples from control and experimental bags (i.e., with and without isotopically labeled D6-DMS), and followed the time-course of m/z 62 and 68 over ~6 h.

In our DMS GP experiments, where D6-DMS is added at > 200 times the concentration of natural DMS, a small secondary source of m/z 62 DMS results from ion source fragmentation of the added competitive inhibitor. We thus corrected the measured m/z 62 DMS signal for one percent mass fragmentation from the D6-DMS (http://webbook.nist.gov/; Table 1, Eq. 1). Note that this fragmentation process is a characteristic of the mass spectrometer ion source and is expected to remain constant as long as ionization conditions (e.g., electron energy) remain constant. We calculated the gross and net DMS production rate in GP experiments from the slope of the natural logarithm of unlabeled DMS concentrations over time (Table 1, Eqs. 2, 3), using a linear regression of the concentrations during the first three time points. In two (out of ten) experiments, when regressions had $r^2 < 0.5$, or the experiment had gross DMS production less than net DMS production, the data were excluded from further analysis. Gross DMS production was determined from the rate of change of these compounds in samples amended with competitive inhibitors of DMS uptake. Net DMS production was determined from the rate of change of DMS in control samples with no added inhibitors. Inferred DMS consumption was calculated from the difference of the gross and net production rates. Measured rate constants of DMS production and consumption were multiplied by the respective DMS concentrations measured in the starting incubation water to yield estimated in situ rates of DMS production and consumption (nM d^{-1}) during the time of our sampling.

One potential caveat of the gross production experiments is the need to add high concentrations of analog substrates. Although dueterated DMS is not harmful to microorganisms, the addition of excess concentrations of DMS could potentially alter the metabolic behavior of bacteria, zooplankton, and possibly phytoplankton. However, the good agreement between results obtained in competitive inhibitor experiments and tracer studies on 17th Dec 2012 and 15th Feb 2013 and in previous work (Asher et al. unpubl.), where background DMS/P concentrations were not strongly perturbed, suggests that our short-term gross production estimates are reasonable approximations of in situ values.

Stable isotope labeling experiments

Isotope tracer experiments were used to quantify specific DMS production pathways (DMSP cleavage and DMSO reduction) and to measure rates of gross DMS loss. For these experiments, we amended three replicate bags with near tracer level (i.e., < ~20% of ambient) additions of D-3 DMS (i.e., all three H atoms of one CH_3 group replaced by deuterium), D-6 deuterated DMSP, and C-13 labeled DMSO to achieve final concentrations of ≤ 0.7 nM, ≤ 0.5 nM, and ≤ 0.7 nM. Given the analytical capabilities of our quadrupole mass spectrometer (detection limit of ~0.1 nM DMS), we were unable to quantify DMS production and consumption using true tracer level additions of (< 10% ambient concentrations) in environments with ambient DMS/P/O concentrations in the low nM concentration range. As a result, the rates derived using this stable isotope tracer method may represent upper bounds on DMS production and consumption rates in these environments. The derived rates do, however, provide useful information on the relative rates of DMS production from $DMSP_d$ and $DMSO_d$ and the balance DMS production and gross DMS loss. The rate of change in labeled DMS (either D3, D6, or $13C_2$) was measured over 4 time points using PT-CIMS. After DMS sparging, replicate subsamples from time points t_0 and t_4 were treated with 6 mL of 10N NaOH or 6 mL $TiCl_3$ to measure (via PT-CIMS) the concentrations of both labeled and natural DMSO and DMSP, respectively.

A number of steps were required to obtain rate estimates from the raw data obtained in tracer experiments. The equations used for these calculations are summarized in Table 1. We calculated gross DMS loss rate constant from D-3 DMS disappearance, while the rate of $DMSP_d$ cleavage and $DMSO_d$ reduction were derived from the rate constant of formation of D-6 and C-13 labeled DMS, respectively (m/z 68 and m/z 64). The loss rate of D-3 DMS provides an estimate for gross DMS removal, since there is no natural formation process for this labeled species. To calculate the gross DMS loss rate constant, we used a pseudo first-order equation (Table 1, Eq. 4), where k_{dms_cons} is the observed rate constant, t is time, and [D-3 DMS] is the concentration of the added tracer. As the tracer experiments were conducted in UV transparent bags under natural light, k_{dms_cons} represents DMS removal from both photo-oxidation and biological DMS consumption.

In our experimental system, there are two other sources of DMS with a charge to mass ratio of 64, in addition to that produced from 13C-labeled DMSO. The first is attributable to the background pool of S_{34}-containing DMS. Based on the natural abundance of S_{34}, we assume that m/z 64 DMS represents 4.3% of unlabeled DMS pool. The second source of m/z 64 DMS results from ion source fragmentation of m/z 65 DMS from the added D3-DMS tracer. Under the ionization conditions used in our mass spectrometer (electron impact ion source with 70 eV ionization energy), the m/z 64 DMS represents a constant background of ~30% of the m/z 65 pool (http://webbook.nist.gov/). We thus corrected the apparent DMS m/z 64 in our experiments for these two source terms (Table 1, Eq. 5), to calculate the concentration of DMS derived specifically from the reduction of 13C-labeled DMSO. To derive gross rates of DMSO reduction, we took into account the loss rate of $^{13}C_2$ labeled DMS, using

the DMS consumption rate constant measured with the D-3 DMS tracer (Table 1, Eq. 6). Gross $DMSO_d$ reduction rate constants were then computed from the slope of the natural logarithm of corrected m/z 64 DMS against time (Table 1, Eq. 7).

The D6-DMS derived from the cleavage of D-6 $DMSP_d$ has a m/z ratio of 68. To the best of our knowledge, D-6 DMS is the only compound with this m/z ratio and gas chromatograph retention time in our experimental system, so DMS_{68} was not corrected for any background signals. The appearance of D-6 DMS over time in our experiments represents $DMSP_d$ cleavage exclusively. D6-DMS is consumed during these experiments and must be corrected for gross DMS loss as described above (Table 1, Eq. 8). We used the slope of the log-transformed corrected D-6 DMS concentrations over time to calculate the $DMSP_d$ cleavage rate constant (Table 1, Eq. 9).

For all tracer measurements, we assumed initial DMS concentrations of 0.1 nM in cases where the actual values were below our detection limit (e.g., early in the spring season). This assumption was necessary in 8% of (5 out of 60) t_0 measurements, and has only a minor effect on our results. For example, if the actual t_0 concentrations were 10-fold lower than the ~0.1 nM detection limit (i.e., ≤ 0.01 nM), derived rate constants (d^{-1}) would be between 3% and 20% higher. As with CI experiments, DMS production rates from tracer studies were determined using a linear regression of log-transformed concentrations against time during the first three time points, and measured rate constants were multiplied by the average DMS/O/P concentration at t_0 to estimate in situ rates (nM d^{-1}).

Microzooplankton dilution experiments

We conducted five dilution experiments between December and February, following the method of Landry and Hasset (1982) and Landry et al. (1995), with a few modifications as suggested by Salo et al. (2010). Seawater was sampled from 10 m depth at dusk from Station B using Niskin bottles and immediately returned to the laboratory for subsequent processing in the 4°C acid-cleaned cold room. A portion of the collected water was filtered as slowly as possible through a 0.1 μm cartridge using acid-clean silicone tubing to minimize the release of DMSP and DMS during the filtration step (see below for details), and added in varying amounts to 1 L acid–cleaned (soaked overnight in 10% HCl) polycarbonate bottles. The residual volume of the 1 L bottles was filled with the unfiltered seawater collected from Station B, yielding duplicate bottles containing 100%, 75%, 50%, and 25% unfiltered water without any headspace. These replicates were spiked with nutrient additions (10 μM nitrate and 0.6 μM phosphate). To measure the background production rate of chlorophyll *a* (Chl *a*) and DMSP, one additional pair of bottles was filled only with unfiltered water without added nutrients. All of the bottles were placed upright in an outdoor incubator with two layers of neutral density coarse mesh screening and flowing surface seawater.

A potential caveat of DMS production estimates in dilution experiments is the potential release of $DMSP_d$ and DMS during the filtration step (Salo et al. 2010). We measured a maximum difference of 15% between $DMSP_d$ and DMS levels in the bulk filtrate and in unfiltered seawater. For example, on 9 Feb during a small *phaeocystis* bloom, we measured 2.4 nM and 2.7 nM of DMSPd and 8.7 nM and 9.6 nM of DMS in the unfiltered and filtered seawater, respectively. We thus conclude that filtration artifacts did not likely introduce significant changes in sulfur concentrations in our experiments.

Initial t_0 levels of Chl *a*, bacterial abundance, and sulfur compounds in dilution water were sampled at the start of incubations, using pre-cleaned syringes and Teflon tubing. Chl *a* concentrations were measured using fluorometric analysis on 200 mL GF/F filtered samples, and bacterial abundance was measured using flow cytometric analysis (see ancillary measurements in the Supporting Information for details). The t_0 values for Chl *a*, DMS, $DMSP_t$, and $DMSP_d$ in each experimental bottle were computed from the dilution fraction and the t_0 values in the bulk filtered and unfiltered samples. After 24 h, duplicate bottles were removed from the incubator and sampled for Chl *a*, bacterial abundance, $DMSP_t$, $DMSP_d$, DMSO, and DMS (t_{24}). The Chl *a*-based specific growth rate in each bottle ($k_{\mathrm{Chl}\ a}$) was calculated as the natural logarithm of Chl a_{t24}/Chl a_{t0}, while the grazing rate (Chl a_{graz}) was calculated from a Type I linear regression of $k_{\mathrm{Chl}a}$ against the dilution fraction (Landry and Hasset 1982; Landry et al. 1995). The DMSP removal rate due to grazing ($DMSP_{graz}$) was calculated using a Type I regression of the natural logarithm of $DMSP_{p\_t24}$/$DMSP_{p\_t0}$ against the dilution fraction (Salo et al. 2010). We calculated the fraction of DMS produced due to DMSP grazing (DMS_{prod_fract}) using a Type II linear regression of the change in DMS concentrations over 24 h (DMS_{T24}–DMS_{T0}) against the quantity of DMSP removed during the experiment ($DMSP_{t\text{-}t24}$–$DMSP_{t\text{-}t0}$). This approach differs from Salo et al. (2010), who used an exponential equation to calculate the net change in DMSP over the 24-h period. We believe that our approach is justified because the model of Salo et al. (2010) assumes that $DMSP_p$ is directly correlated to the phytoplankton growth rate (which it is often not). Our simplified approach does not make this assumption. Finally, we calculated the rate of DMS production attributable to micrograzing by multiplying $DMS_{prod\_\ fract}$ by $DMSP_{graz}$.

To minimize sample perturbations, we did not add stable isotope tracers to the microzooplankton dilution experiment bottles. Tracer additions in these experiments would have enabled us to quantify changes in DMSP cleavage or gross DMS loss rates across the dilution gradient, examining potential density-dependent artifacts. In the absence of

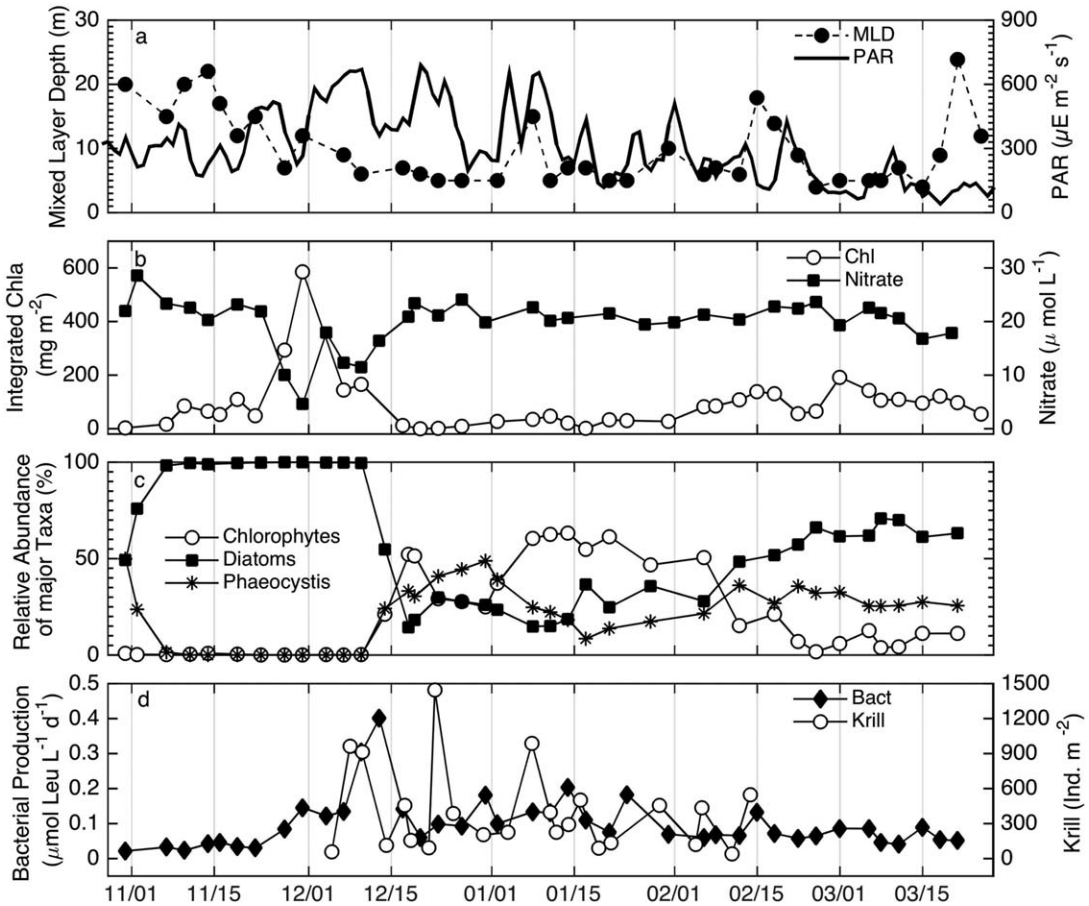

Fig. 2. Time-series of (**a**) mixed layer depth (MLD; derived from a density difference criterion, $\Delta\sigma_t$, of 0.125 kg m^{-3}), and daily averaged photosynthetically active irradiance (PAR), (**b**) depth-integrated Chl *a* and nitrate concentrations, (**c**) relative abundance of diatoms, *Phaeocystis* and chlorophytes at 10 m depth, (**d**) bacterial production and krill abundance. Surface ocean measurements were derived from ~semi-weekly sampling at Station B, as described in the methods.

direct measurements, we (and others—Salo et al. 2010) assume that such density dependence does not have a significant influence on our results. Given the similar levels of DMS and $DMSP_d$ concentrations across the dilution treatments, we expect cell-specific bacterial DMS production and consumption rates in these experiments to have remained similar across treatments. As such, the total (i.e., volumetric) rates of bacterial $DMSP_d$ consumption should scale linearly with the dilution factor, in a manner analogous to grazing rates.

Data obtained from individual micro-grazing experiments were used to derive an estimate of water column DMS production (nM d^{-1}). This estimate was calculated as a product of the rate of DMS production due to grazing (DMS_{prod}), the DMSP removal rate due to grazing ($DMSP_{graz}$) and the in situ $DMSP_p$ concentrations (Table 1, Eq. 10) at Station B. For this analysis, we excluded results from 1 (out of 6) grazing experiment, where Chl *a* concentrations did not show a linear dependence ($r^2 > 0.5$) on the dilution fraction.

Krill grazing experiments

In late February, we conducted three measurements of krill grazing rates during a period of high *E. superba* abundance in the waters around Palmer Station. Experiments were conducted over a 12-h period using Station B water dispensed into six 50 L carboys. The carboys were filled at local dusk with water from below the mixed layer (~20 m depth) using a Monsoon pump. We spiked the carboys with 1 L of tracer spike solution containing 1 L of seawater from ~20 m depth collected when the carboys were filled, D-3 DMS, and D-6 DMSP to obtain final concentrations of 1.42 nM D-3 DMS and 1.33 nM D-6 DMSP. Carboys were then transported back to Palmer Station for further processing. On station, the carboys were sampled for initial (t_0) measurements of Chl *a*, DMS/P_d and $DMSP_t$ in 50 mL subsamples sampled using syringes and clean teflon tubing. Isotopically labeled DMS was analyzed via PT-CIMS (as described above), and samples were then treated with 10 N NaOH and left for ~12 h prior to DMSP analysis (PT-CIMS).

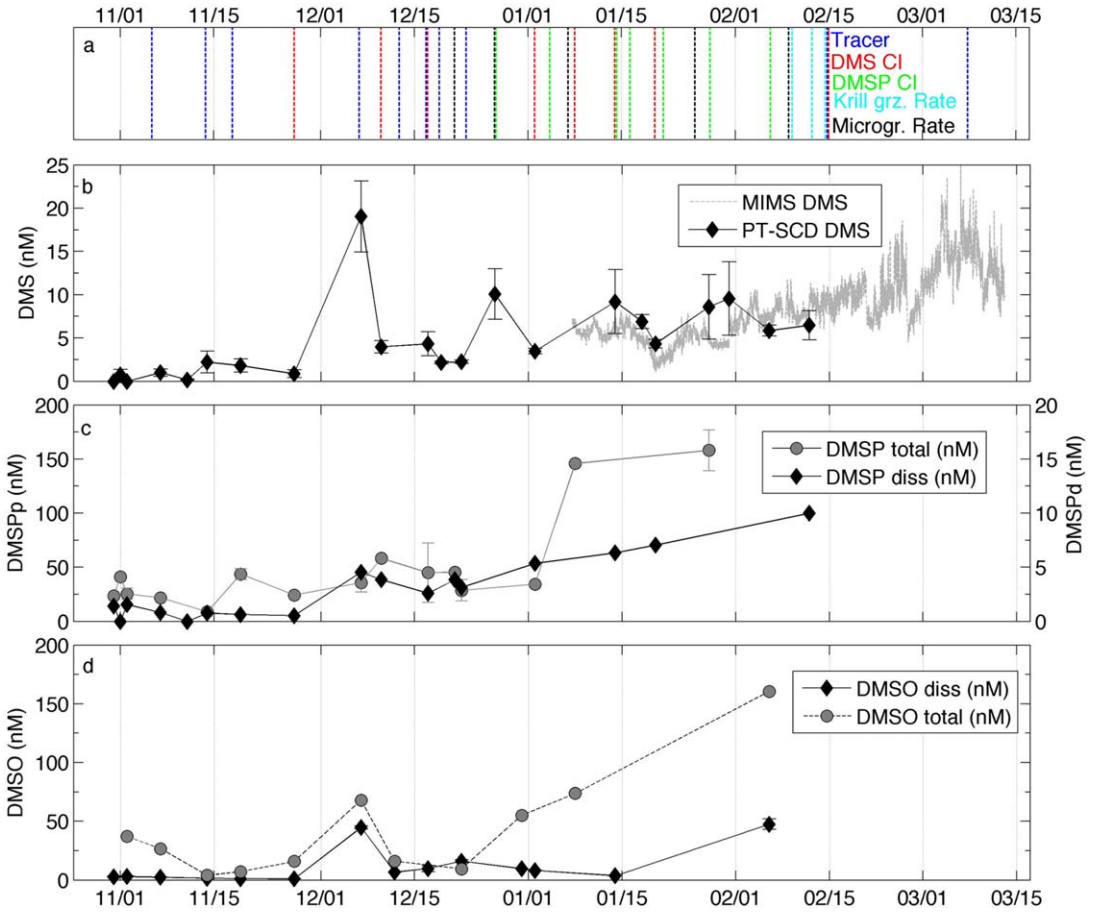

Fig. 3. Time course of sampling activities and DMS/P/O concentrations at Palmer Station. Panel (**a**) shows the sampling dates for various processes studies and rate measurements. Panel (**b**) shows DMS concentration measurements from continuous MIMS analysis of the seawater supply, and discrete measurements at station B (10 m depth). Panels (**c**) and (**d**), show semi-weekly DMSP and DMSO total and dissolved concentrations at station B (10 m depth). Note that axes for total and dissolved DMSP in panel c have different scales.

After these t_0 measurements, we added 10 juvenile krill to three of the six carboys to study the impact of krill on $DMSP_p$ grazing, net DMS production, rates of $DMSP_d$ cleavage, and rates of DMS consumption. The other three carboys served as experimental controls. Krill added to the carboys were obtained from net tows (700 μm mesh diameter) deployed from a zodiac equipped to locate krill using acoustic measurements. Carboys were capped, sealed with parafilm and moved to the outdoor flow-through incubator, where they were slowly rotated every 3 h to prevent the phytoplankton from settling to the bottom. After 24 h, the carboys were removed and sampled a second time for Chl *a*, DMS, and DMSP.

We calculated the net change in DMS, $DMSP_{p/d}$ and Chl *a* over the course of the krill grazing experiments. Error estimates for each rate measurement were calculated as the standard error of triplicate rates (DMS/P or Chl *a* d^{-1}). Mean DMS production in these experiments was normalized to the abundance of krill in our experiments (10 krill in a 50 L carboy = 0.2 krill L^{-1}). These krill-specific DMS production rates were then used to derive an estimate of the depth integrated in situ DMS production from krill grazing (Table 1, Eq. 11). For this computation, krill-specific DMS production rates were multiplied by the krill densities (ind. m^{-3}) derived from acoustic measurements (ind. m^{-2}; Kim Bernard pers. comm.) and the mean bathymetric depth of our study area (~88 m; Fig. 1). This estimate assumes a uniform DMSP concentration in the mixed layer (derived from measurements at one depth) and little or no DMSP below the mixed layer. The assumption could lead to an underestimate of DMS production from Krill grazing, particularly in late February and March when a deep *Phaeocystis* bloom was observed below the mixed layer. Indeed, results from one depth profile in late January revealed substantial accumulations of $DMSP_t$ below the mixed layer (~55 nM) that support this interpretation (data not shown). Sub-mixed layer accumulation of DMSP would lead to an underestimate in our estimates of DMS production from krill grazing.

Table 2. Pearson correlation coefficients between DMS/P/O concentrations at Station B and ancillary measurements over the seasonal cycle. Significance level indicated by * for $p < 0.05$, ** for $p < 0.01$, and *** for $p < 0.001$.

	DMS	$DMSP_d$	$DMSP_t$	$DMSO_d$	$DMSO_t$
$DMSP_d$	0.54*				
$DMSP_t$	0.34	0.42			
$DMSO_d$	0.75**	0.47	0.27		
$DMSO_t$	0.41	0.31	0.66	0.78**	
MLD	−0.43*	−0.65**	−0.19	−0.36	−0.23
Chl *a*	0.07	−0.05	−0.11	0.15	−0.05
Phaeo	0.27	0.67**	0.85***	−0.01	0.39
UV	0.23	−0.03	0.25	0.35	0.05

Inferring total DMS production/consumption terms

We estimated semi-weekly values for total DMS production and consumption rates using our rate measurements and computed sea-air fluxes (Table 1, Eq. 12). The following specific rates were included in the total DMS production term: (1) $DMSP_d$ cleavage, (2) $DMSO_d$ reduction, (3) DMS production due to microzooplankton, and (4) DMS production due to krill grazing. The DMS loss term was comprised of gross DMS loss from both biological and photo-chemical processes. DMS removal from sea-air flux was also included (see Supporting Information for details of the calculations). Dissolved DMS loss rates were derived from gross DMS loss measured in tracer experiments and inferred gross DMS loss in CI experiments. We calculated the uncertainty for each term from the standard error of the derived rate constants and concentration measurements. Where necessary (i.e., DMS production/consumption rates), uncertainty was propagated using a Taylor Series expansion.

Results

Surface water hydrography and plankton biomass

Our field campaign captured a significant portion the seasonal cycle (late spring, summer, and early fall) at Palmer Station in 2012/2013 (Fig. 2). By 16 Nov 2012, sea ice had retreated, exposing surface waters to increased gas exchange. Over the course of the seasonal cycle, the mixed layer shoaled from ~20 m to ~8 m (Fig. 2a), while average daily surface PAR levels increased to ~600 $\mu E\ m^{-2}\ s^{-1}$, resulting in a significantly increased mixed layer mean irradiance.

In late November, we observed a massive diatom-dominated phytoplankton bloom that achieved peak Chl *a* levels in excess of 600 mg m^{-2} (26 $\mu g\ L^{-1}$), and coincided with the drawdown of ~30 μM nitrate in surface waters (Fig. 2b,c). This spring bloom crashed within 2 weeks, and nitrate levels were restored to 20 μM (Fig. 2b), likely due to the advection of surface waters offshore and vertical entrainment of Upper Circumpolar Deep Water, as discussed by Tortell et al. (2014). Following the initial diatom bloom, relatively low phytoplankton biomass persisted for 2 months (Fig. 2b), with the assemblages containing a mixture of chlorophytes, diatoms and *Phaeocystis* (Fig. 2c). Given elevated macronutrient concentrations and high photosynthetic efficiency during this period (as measured by variable Chl *a* fluorescence, F_v/F_m; Tortell et al. 2014), we presume that top-down controls were responsible for this period of low phytoplankton biomass following mid-December. In February, a second, smaller phytoplankton bloom developed (Fig. 2b), which was comprised of a mixture of diatoms and *Phaeocystis* (Fig. 2c). CTD-based Chl *a* fluorescence data suggested that this latter bloom was largely located below the mixed layer (Tortell et al. 2014). Krill biomass fluctuated significantly during our sampling period, with sporadic increases of *E. superba* observed at various times between December and February, reflecting patchy distributions over short time and space scales (Fig. 2d). High rates of bacterial production (measured as the incorporation of ^{3}H-Leucine; Simon and Azam 1989; Smith and Azam 1992; Goldman et al. 2015) were observed directly following the crash of the spring bloom (Fig. 2d), with smaller periodic increases observed through mid-February.

DMS/P/O concentrations

DMS concentrations, measured semi-weekly at Station B, fluctuated throughout the seasonal cycle, with an overall mean of 4.7 ± 4.6 nM, and a range from < 0.1 nM (detection limit) to 19 nM (Fig. 3b). The largest, albeit short-lived, DMS peak also occurred early-December, and may have coincided with the peak in Chl *a* concentrations (unfortunately we lack DMS/P/O measurements on the date of the Chl *a* maximum). In general, high frequency MIMS DMS measurements from the SWP showed good coherence with DMS measurements Station B for the period of overlap, with a maximum offset of 2 nM between the two data sets. The MIMS data also provide additional, high frequency DMS observations (see below) through to the end of our sampling period after discrete measurements had stopped. The MIMS data suggest that surface DMS concentrations continued to climb throughout February (after semi-weekly measurements had ceased), with a decreasing trend by early March. DMS concentrations measured at Station B were weakly (though statistically significantly) correlated with the mixed layer depth ($r = -0.43$, $p < 0.05$; Table 2). In contrast, DMS concentrations at Station B did not show any significant correlations with Chl *a*, the abundance of *Phaeocystis*, PAR, or UV (Table 2).

$DMSP_t$ concentrations at Station B did not exceed ~60 nM for the majority of the season (mean 49.3 ± 43.4; Fig. 3c), although very high concentrations (~150 nM) were observed during the final two sampling points in late February (Fig. 3c). Measurements were not obtained after this time due to instrument problems. $DMSP_t$ concentrations were closely coupled to the abundance of *Phaeocystis* ($r = 0.85$, $p < 0.001$; Table 2). $DMSP_d$ remained < 2 nM during the early part of our sampling (until December), after which concentrations began to

Table 3. DMS production and removal terms (nM d^{-1}) calculated from in situ measurements and experimental rates (see Table 1 for equations). Standard error terms were calculated using standard error propagation of the standard error in specific rate constants measurements and concentration measurements. Specific rate constants were calculated as the mean of rate constants derived from each replicate or incubation bottle. Rate constants lower than our detection limit (<0.2 d^{-1}) are denoted by n.d. Short dashes indicate a lack of data.

Dates	DMSP cleavage (nM d^{-1})	DMSO reduction (nM d^{-1})	Microzoop. grazing (nM d^{-1})	Krill grazing (nM d^{-1})	Gross DMS loss (nM d^{-1})	Sea-air flux (nM d^{-1})
06 Nov	1.6 ± 0.83	1.6 ± 1.1	-	-	−2.5 ± 2.4	−0.88 ± 0.0
18 Nov	0.78 ± 0.70	n.d.	-	-	n.d.	−1.4 ± 0.74
27 Nov	-	-	-	-	−0.72 ± 1.2	−0.33 ± 0.12
07 Dec	0.44 ± 0.33	n.d.			−1.2 ± 0.81	−0.64 ± 0.26
13 Dec	n.d.	4.28 ± 2.2	-	0.38 ± 0.32	−19 ± 6.9	−2.1 ± 0.73
17 Dec	-	-	-	0.10 ± 0.04	−0.52 ± 0.8	−2.9 ± 1.0
19 Dec	8.6 ± 8.0	n.d.	-	-	−2.2 ± 1.0	−0.92 ± 0.08
20 Dec	-	-	2.0 ± 1.2	0.30 ± 0.25	-	−0.74 ± 0.07
23 Dec	17 ± 3.3	13 ± 2.4			−38 ± 11	−0.43 ± 0.10
27 Dec	-	-	-	-	−21 ± 15	−0.91 ± 0.10
31 Dec	-	-	1.5 ± 0.46	0.93 ± 0.77	-	−0.55 ± 0.07
02 Jan	-	-	-	-	−25 ± 14	−1.4 ± 0.03
06 Jan	-		8.1 ± 4.6	1.0 ± 0.85	-	−4.8 ± 1.9
14 Jan	-	-	-	1.0 ± 0.86	−25 ± 16	−9.3 ± 4.3
21 Jan	-	-	-	0.13 ± 0.11	-	−4.2 ± 1.1
26 Jan	-	-	5.7 ± 3.5	0.96 ± 0.81	-	−6.00 ± 2.78
09 Feb	-	-	11 ± 4.6	0.94 ± 0.79	-	−4.65 ± 1.23
15 Feb	16 ± 12	n.d.	-	-	−9.7 ± 1.7	−7.0 ± 2.1
08 Mar	n.d.	n.d.	-	-	−5.7 ± 1.9	−3.6 ± 1.8

accumulate to values as high as 10 nM by mid February. The difference between $DMSP_t$ and $DMSP_d$ suggests that phytoplankton contained substantial concentrations of particulate DMSP. Although $DMSP_d$ concentrations were not significantly correlated with $DMSP_t$ ($r = 0.42$, $p = 0.15$; Table 2), DMS concentrations did track $DMSP_d$ concentrations at Station B ($r = 0.54$, $p < 0.05$; Table 2).

During the majority of our study period, $DMSO_t$ concentrations remained lower than $DMSP_t$ concentrations with maximum values not exceeding ~50 nM between November and January. During the end of our sampling period, however, $DMSO_t$ concentrations reached values as high as 150 nM, similar to the observed $DMSP_t$ concentrations (Fig. 3c). During the first half of our sampling season, $DMSO_d$ encompassed the bulk of the $DMSO_t$ pool, suggesting a low concentration of $DMSO_p$. In contrast, during latter half of sampling season (February and March) the large increase in the $DMSO_t$ pool was not accompanied by a commensurate increase in the $DMSO_d$ pool, suggesting the accumulation of a particulate DMSO pool towards the end of our sampling period. Despite the decoupling between $DMSO_d$ and $DMSO_t$ during the late season, these two pools were well correlated in our full data set ($r = 0.78$, $p < 0.01$; Table 2). The $DMSO_d$ pool size was also significantly correlated with DMS concentrations ($r = 0.75$, $p < 0.01$; Table 2).

Rate measurements and process studies

In isotope tracer experiments, we simultaneously measured rates of $DMSP_d$ cleavage, $DMSO_d$ reduction, and gross DMS loss. Supporting Information Figure S1 shows an example of the raw data obtained from a tracer experiment on 23 Dec 2012. Table 3 shows the derived rates (nM d^{-1}) of these various processes across our full sampling season. $DMSP_d$ cleavage rate constants averaged 2.7 ± 0.50 d^{-1} (range 0.31–3.9 d^{-1}), $DMSO_d$ reduction rate constants averaged 1.6 ± 0.57 d^{-1} (range 0–5.1 d^{-1}) and gross DMS loss rate constants averaged 3.8 ± 1.7 d^{-1} (range 0.41–12 d^{-1}). Table 3 also shows the rates of gross DMS loss calculated over the sampling season derived from CI experiments (see Supporting Information Fig. S2 for an example of the data from CI experiments). The CI experiments also yielded rapid and variable rate constants of gross DMS production (mean 1.5 ± 1.3 d^{-1}; range 0.10–2.8 d^{-1}), and net DMS change. Rate constants of net DMS change (0.13 ± 0.35 d^{-1}; range −0.27–0.86 d^{-1}) were 10-fold lower than rates of gross DMS production. From the difference in measured gross DMS production and

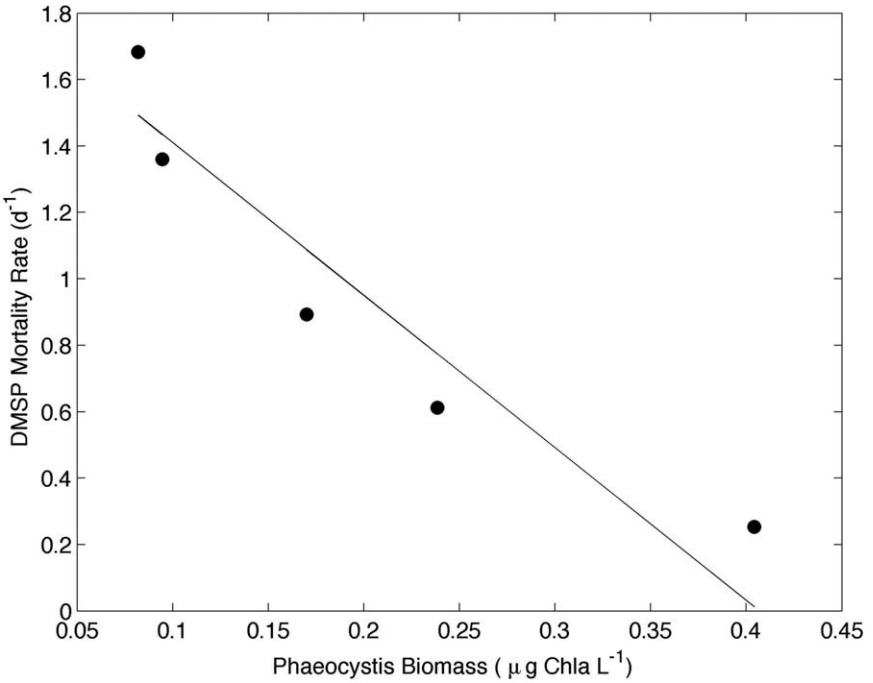

Fig. 4. Relationship between the abundance of *Phaeocystis* biomass and the DMSP loss rate observed in five micro-grazing experiments. The abundance of *Phaeocystis* was calculated by scaling the ancillary marker pigment 19′hex (μg 19′hex L^{-1}) by 1.25, according to an algorithm developed for the Southern Ocean by Everitt et al. (1990) and implemented more recently by Goldman (2015). The line represents the Type II linear regression line ($DMSP_{rem} = -4.6 \pm 0.73$ (Phaeo) $+ 1.9 \pm 0.17$; $r^2 = 0.89$) calculated using the MATLAB script lsqfitma from Glover et al. (2011).

net DMS production rates in GP experiments, we calculated gross DMS loss rates (mean $= 1.7 \pm 0.53$ d^{-1}; range 0.26–3.2 d^{-1}; Table 3. Parallel rate measurements on 17th Dec 2012 and 15th Feb 2013 using the GP technique and stable isotope tracer technique yielded consistent results. On 17th Dec, using the GP technique, we observed that DMS loss rates that were not significantly different from zero (-0.27 ± 0.40 d^{-1}), while DMS loss rates were below the detection limit in our tracer experiment (n.d.). Similarly on 15th Feb, using the GP technique, we observed that DMS loss rates were 2.4 ± 0.40 d^{-1} and, while DMS loss rates were 1.2 ± 1.0 d^{-1} in our tracer experiment. Compared with the highly variable rates of DMS production and consumption, we found that gross DMSP production rate constants (derived from Glycine Betaine DMSP GP experiments) remained fairly constant over the season (2.4 ± 0.23 h^{-1}; data not shown).

Grazing experiments

Typical results from one micro-grazing experiment on 07 Jan 2013 are presented in Supporting Information Fig. S3, while Table 4 shows the results obtained from five independent micro-grazing experiments, conducted between late December and early February These repeated experiments showed Chl *a* mortality rate constants ranging from 0.1 to 0.2 d^{-1}, with larger grazer effects of grazing on $DMSP_p$ (range 0.25–1.7 d^{-1} removal rate constants). As the summer progressed and the phytoplankton community composition shifted to a community composition comprising mixed *Phaeocystis* and diatom assemblages (Fig. 2), the grazer effects on DMSP and Chl *a* removal decreased (Table 4). Indeed, the grazing effect on DMSP removal exhibited a strong negative relationship with the abundance of *Phaeocystis* (Fig. 4; $r = -0.94$, $p < 0.05$, $n = 5$). For most of the experiments (four out of five), we measured a ratio of DMS production and DMSP removal less than 0.15 (Table 4). In the final experiment, however, (09 Feb), this ratio was close to 1, suggesting that almost all of the DMSP removed by grazing was being converted to DMS (Table 4). We observed a positive correlation between *Phaeocystis* abundance and DMS production associated with DMSP removal (Type II regression $r = 0.92$, $p < 0.05$, $n = 5$).

Results from three 24-h krill grazing experiments demonstrated that krill could significantly influence net $DMSP_p$ removal and DMS production (Fig. 5). On average, the presence of krill resulted in a significant increase in net DMS accumulation from 4.7 ± 3.4 nM in control treatments to 12 ± 2.2 nM and a significant decrease in net $DMSP_t$ accumulation from 18 ± 7.1 in control treatments to -9.1 ± 9.8 nM. As expected, net Chl *a* accumulation also decreased on average in the presence of krill (Fig. 5). In all three experiments, we observed higher $DMSP_d$ cleavage rates (calculated from changes in m/z 68 DMS) and lower gross DMS loss rates (calculated from changes in m/z 65 DMS) between krill and

Table 4. Effects of microzooplankton grazing on Chl *a* and DMSP loss rates and DMS production measured in 24 h dilution experiments. Chl *a* and DMSP loss rates were calculated from the slope of the natural logarithm of the ratio of final and initial Chl *a* and DMSP vs. the fraction of filtered (i.e., grazer-free) seawater. DMS produced from grazed DMSP is calculated from the net change in DMS concentrations over time normalized to DMSP loss. Error bars represent standard errors of the means.

Date	Chl *a* mortality Rate (d^{-1})	DMSP mortality Rate (d^{-1})	mol DMS prod/ mol DMSP grazed
21 Dec	0.20 ± 0.08	1.36 ± 0.15	0.09 ± 0.06
28 Dec	0.20 ± 0.06	1.68 ± 0.30	0.04 ± 0.01
07 Jan	0.21 ± 0.05	0.61 ± 0.09	0.14 ± 0.04
26 Jan	0.09 ± 0.01	0.89 ± 0.32	0.14 ± 0.01
09 Feb	0.10 ± 0.02	0.25 ± 0.02	0.96 ± 0.12

control treatments. On average, the differences in DMSP cleavage, 6.1 ± 1.6 nM and 8.6 ± 3.1 nM and DMS loss, −5.7 ± 3.5 nM and −3.6 ± 1.9 nM in control and krill treatments, respectively, were sufficient to explain the observed elevated net DMS production in the presence of krill (Fig. 5). In addition, we also measured high DMS/P content in the fecal matter and krill bodies from experimental treatments in the second experiment (Supporting Information Table S1). We note that the contribution of krill grazing to DMS/P cycling in natural waters (Table 3) depends on krill abundance in the water column, which varied significantly over the course of our field study (Fig. 2c).

Seasonal trends in DMS production/consumption

Rate of DMS production derived from tracer and grazing experiments, varied considerably over the seasonal cycle (Table 3). We observed low initial rates of $DMSP_d$ cleavage that increased rapidly following the spring bloom to reach maximum rates > 15 nM d^{-1} by mid-December (Table 3). Specific rate constants of $DMSP_d$ cleavage (d^{-1}) increased rapidly during the post-bloom period (Fig. 6), and were negatively correlated (Type II regression; $r = -0.89$, $p < 0.05$; $n = 6$) with net primary production as measured by Goldman et al. (2015). Following the decline of the phytoplankton bloom in December, DMS production rates from microzooplanton grazing (8.1 ± 1.5 nM d^{-1}) became an important DMS source for the remainder of the austral summer. During most of sampling season, $DMSP_d$ cleavage and microzooplankton grazing dominated total DMS production, with smaller contributions from krill grazing and sporadic contributions from $DMSO_d$ reduction (Table 3). Low in situ DMS production due to krill grazing reflects the patchy distributions of krill in the water column (Fig. 2c; Table 3).

Gross DMS loss rates from tracer and CI experiments also reached a maximum after the spring bloom in December (38 ± 11 nM d^{-1}; Table 3). Figure 6 shows the derived rate constants for gross DMS loss, which peaked in mid-December, during a post spring-bloom period of maximum bacterial production. Across our full seasonal sampling, we observed a correlation between specific rates of gross DMS loss and bacterial production (Type II regression; $r = 0.72$, $p < 0.01$; $n = 12$). Rate constants for gross DMS loss were not correlated with rate constants from $DMSP_d$ cleavage (Fig. 6). Measured gross DMS loss rates were > 10 times higher than DMS removal calculated for sea-air flux in the spring and early summer (Table 3), suggesting that biological and photo-chemical DMS consumption dominated DMS removal. By late summer, however, sea-air flux appeared comparable to gross DMS loss rates (Table 3).

Seasonal DMS budget

In addition to examining seasonal changes in the various DMS production and consumption terms, we also computed overall means for rates of $DMSP_d$ cleavage, $DMSO_d$ reduction, gross DMS loss, sea-air flux, mircro-zooplankton grazing, and krill grazing (Fig. 7). This analysis showed that multiple sources of DMS were required to balance gross DMS loss from bacterial and photochemical processes, as well as sea-air flux in the seasonal DMS budget. Average rates of DMS production over the seasonal cycle ranked as follows: (1) microzooplankton grazing, (2) $DMSP_d$ cleavage, (3) $DMSO_d$ reduction, and (4) krill grazing. Over the seasonal cycle, the mean net balance of our rate measurements was slightly positive but not significantly different from zero (Fig. 7).

Discussion

The new observations presented here increase our understanding of seasonal variability of DMS, and the related compounds DMSP and DMSO in coastal Antarctic waters. Beyond contributing to a growing database of DMS concentration measurements in the WAP region, our work adds a new dimension, with the first data on DMSO concentrations and turnover in this region, and the use of multiple experimental approaches to quantify DMS production/consumption terms.

Seasonal variability

The concentrations of DMS and DMSP we observed during this study agree with previously published values at Palmer Station (Fig. 1; Berresheim et al. 1998; Herrmann et al. 2012), which exhibit similar mean values and ranges. The few available data from Palmer Station suggest that spring/summer DMS concentrations in this region average ~5 nM, ranging from < 1 nM to ~20 nM, with several peaks over the seasonal cycle (Berresheim et al. 1998; Herrmann et al. 2012). Limited overlap exists between this study and previous studies, which did not explicitly measure rates of DMS production from any source. Yet, we can compare DMS loss rates between our study and that of Hermann et al. (2012). Turnover rates derived from our stable isotope tracer and gross DMS production experiments (3.3 ± 0.95 d^{-1}) were

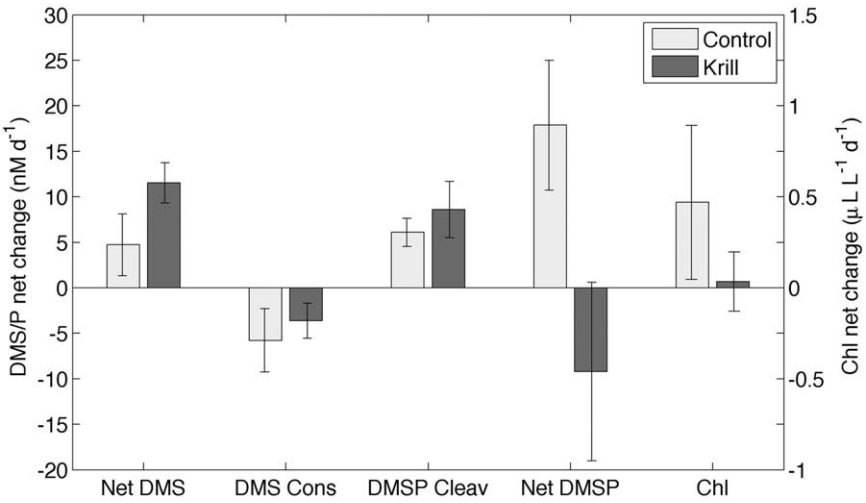

Fig. 5. Derived mean values of net DMS production, gross DMS loss, DMSP cleavage, net DMSP production, and net chlorophyll production in three krill grazing experiments in mid-February. Error bars represent one standard error from the mean. See methods for details on the derivation of the various rates.

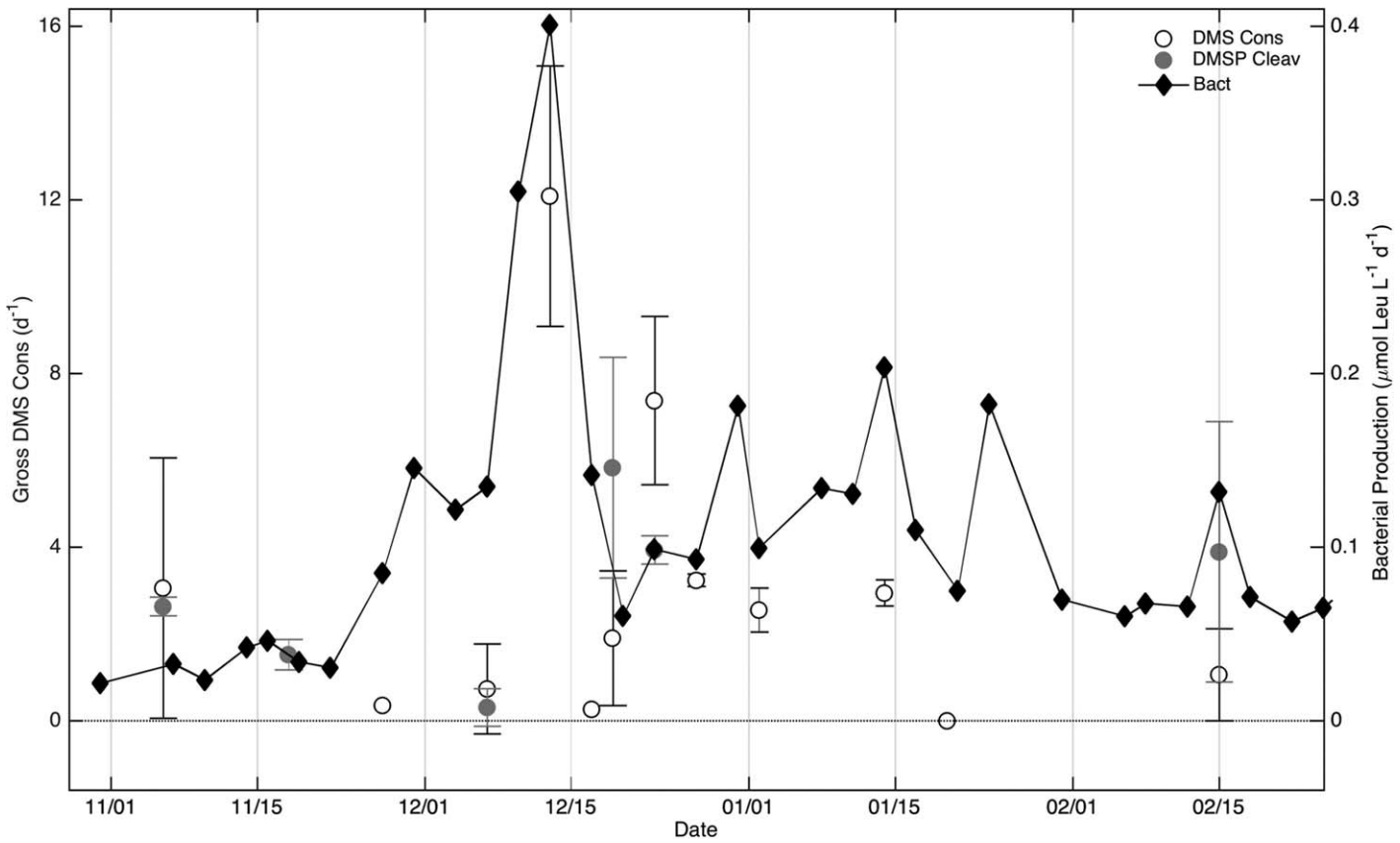

Fig. 6. Comparison of specific rates of DMS cleavage, gross DMS loss and bacterial production over the seasonal cycle. Error bars represent the standard error of the means.

significantly higher on average, and more variable than rate constants measured in 2006 using the radio isotope method (0.71 ± 0.15 d^{-1}; Hermann et al. 2012). Notwithstanding potential discrepancies between these methods, there are several potential explanations for the relatively high rates we observed.

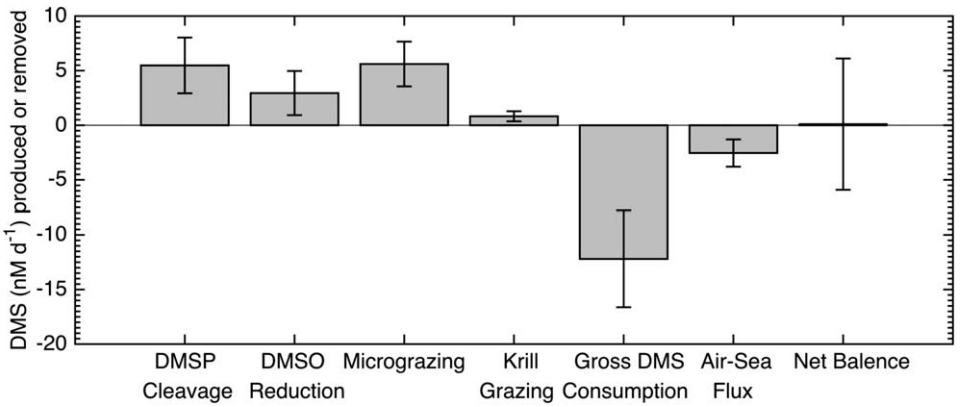

Fig. 7. Seasonal mean rates of DMS production and removal due to $DMSP_d$ cleavage, $DMSO_d$ reduction, micrograzing krill grazing gross DMS loss (biological DMS consumption and photo-oxidation) and air-sea flux. Error bars represent the standard error of all individual rates measured over the seasonal cycle. The net balance term represents the sum of all (mean) DMS production terms minus the sum of all measured (mean) DMS loss terms.

Figure 8 highlights the differences in winter sea ice cover, and in the timing of the phytoplankton blooms at Palmer Station in 2012 and 2006, during our field season and that of Hermann et al. (2012). These differences suggest considerable inter-seasonal variability (potentially reflecting longer-term change in this rapidly warming region) between 2006 and 2012. In the period leading up to our study in 2012, wintertime maximum sea ice cover in the vicinity of Palmer Station was relatively low ($\leq$ 80%) compared to 2006 ($\leq$ 95%). There were also significant differences in phytoplankton biomass dynamics during the two seasons. In 2012, a massive diatom-dominated spring phytoplankton bloom immediately following sea ice retreat in November with Chl *a* as high as 26 mg m^{-3} in surface waters. By comparison, the 2006 spring/summer season was characterized by two successive phytoplankton blooms each with Chl *a* concentrations of $\sim$20 mg m^{-3}.

In 2006 a phytoplankton bloom of mixed assemblage, including phaeocystis, developed in late December, followed by a diatom-dominated bloom in late January (Patricia Martrai pers. comm.). The demise of this first phytoplankton bloom did not coincide with a spike in bacterial production or respiration (data not shown), and DMS concentrations remained $>$ 8 nM for the first 10 d in January, following the crash of the bloom (Patricia Martrai pers. comm.). Conversely, the crash of the large diatom-dominated bloom in early December 2012 likely released substantial DOC (and DMSP), which fueled a rapid increase in bacterial production (Fig. 2). Our data show that sharp increase in bacterial production following the demise of the 2012 phytoplankton bloom was associated with high and variable specific rate constants of gross DMS loss, and a sharp decline in DMS concentrations (Figs. 3, 6). An additional difference between the 2006 and 2012 seasons may have resulted from the lower relative winter sea ice cover between these years. Difference in sea ice dynamics has been shown to influence phytoplankton and zooplankton dynamics (Ducklow et al. 2013), with potential implications for DMS production.

To date, there have been no reports of extraordinarily high (up to $\sim$100 nM) DMS levels in the WAP, in contrast to several Antarctic polynya systems, where such extreme concentrations have been repeatedly observed (e.g., DiTullio and Smith 1995; Tortell et al. 2012). Below, we discuss a number of factors that may lead to the relatively low DMS/P concentrations in WAP, relative to other Antarctic waters. Although there are no comparable DMSO data available from previous studies at Palmer Station, our results indicate that phytoplankton did not accumulate large quantities of intracellular DMSO (DMSOp), relative to DMSP, and this compound was a relatively minor contributor to the total reduced sulfur pool for much of the season. Either cells rapidly exuded $DMSO_p$ into the dissolved pool, or did not produce DMSO directly. The correlation between $DMSO_d$ and DMS concentrations supports the hypothesis that DMS is the main precursor of $DMSO_d$ in surface waters due to the photochemical and biological oxidation of DMS.

Correlations between concentrations of DMS/P and ancillary variables (Table 2) suggest that phytoplankton species composition and water column stratification exert strong controls on DMS/P dynamics. We observed a strong correlation between $DMSP_t$ and the abundance of *Phaeocystis* (Fig. 2), a well-known DMSP producer in Antarctic waters (Stefels et al. 2007). It is thus possible that the lack of massive DMS accumulation in the WAP results from the lower absolute abundance of *Phaeocystis*, as compared to the Ross and Amundsen Sea polynyas (e.g., DiTullio and Smith 1995; Tortell et al. 2012). Based on previous studies (Arrigo et al. 1999), the relatively shallow mixed layer depths observed in the WAP region may have favored diatom growth, thereby limiting DMS accumulation in surface waters. From a physiological perspective, however, shallow mixed layer depths

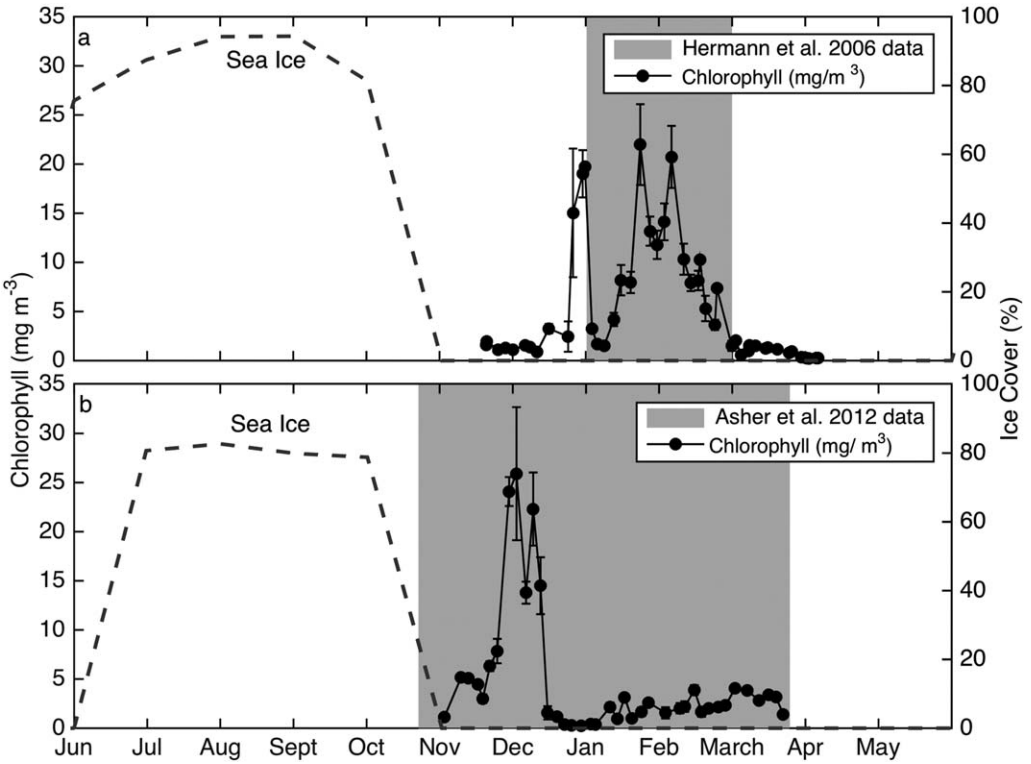

Fig. 8. Comparison of mean sea ice cover (publicly available at http://oceaninformatics.ucsd.edu/datazoo/data/pallter/datasets) and the station B Chl *a* concentrations in (**a**) 2006 when data were collected for the Hermann et al. (2012) study and in (**b**) 2012 when data were collected for this study. Error bars for Chl *a* represent the stand error of measurements.

may act to promote enhanced DMS production by existing phytoplankton by stimulating oxidative stress (Sunda et al. 2002; Vallina and Simo 2007). Indeed, we observed a weak negative correlation between DMS and mixed layer depth during our sampling season. We thus suggest that phytoplankton taxonomic composition exerts a first-order control on surface water DMS/P accumulation in the WAP, with mixed layer depth and irradiance exerting a secondary physiological control. A similar hypothesis has recently been proposed in polar Arctic regions (Levasseur 2013).

Summary of rate measurements

To the best of our knowledge, our measurements of $DMSP_d$ cleavage, $DMSO_d$ reduction, DMS production due to krill grazing, and DMS production due to microzooplankton grazing are the first of their kind for the WAP region. As discussed above, previous measurements of gross DMS loss rate constants (0.71 ± 0.15 d^{-1}) (Herrmann et al. 2012) fall within the (relatively wide) range of our gross DMS loss measurements (0.27–12 d^{-1}) over the seasonal cycle. Whereas the majority of the season was characterized by relatively balanced DMS sources and sinks terms (Table 3), DMS production and consumption terms peaked in mid-December, following a massive diatom bloom. Specific rate constants for gross DMS loss peaked first, and were related to bacterial activity, which was stimulated during the post-bloom period, potentially by the increased availability of organic carbon (Kiene et al. 2000; Galindo et al. 2015). Specific rate constants for $DMSP_d$ cleavage, which peaked a few days later than the maximum rate constants for gross DMS loss, may be tied to a sharp decrease in primary productivity (Fig. 6) and high $DMSP_d$ concentrations. Below, we examine controls on the different DMS/P production and consumption terms over the seasonal cycle.

Sources of DMS

We measured large DMS production terms from the algal/bacterial $DMSP_d$ cleavage and $DMSO_d$ reduction. On average, $DMSP_d$ cleavage was a major source of DMS production (Fig. 7; Table 3), indicating that $DMSP_d$ was the main precursor of DMS over the seasonal cycle. Indeed, the correlation between DMS and $DMSP_d$, and the consistently high specific rate constants of $DMSP_d$ cleavage, support the idea that $DMSP_d$ cleavage was a dominant DMS production term. In January and February, high $DMSP_d$ pools (>5 nM) also contributed to $DMSP_d$ cleavage rates (>15 nM d^{-1}). Elevated $DMSP_d$ was potentially attributable to increased *phaeocystis* abundance (Table 2), and possibly grazing pressure, high UV, and shallow mixed layers, which could accelerate the intracellular release of $DMSP_p$. The low relative contribution of $DMSO_d$ reduction as a source of DMS contrasts recent observations showing significant rates of $DMSO_d$ reduction in sea-

ice brines (Asher et al. 2011). These high rates were the product of large $DMSO_d$ pools, and rate constants of $DMSO_d$ reduction that were comparable to rate constants for $DMSP_d$ cleavage. Although a handful of studies have documented $DMSO_d$ reduction by both phytoplankton and bacteria (e.g., Vila-Costa et al. 2006b; Spiese et al. 2009), we speculate that environmental conditions (e.g., in sea ice brines) or the presence of particular taxonomic groups of bacteria and algae may determine the importance of this poorly studied DMS production pathway.

It has been suggested that DMS production may be increased when algal cells have a physiological history of nutrient stress, growth is limited, and cells accumulate internal pools of sulfur intended for protein synthesis (Stefels et al. 2007). In support of this hypothesis, we observed the highest rate constants of $DMSP_d$ cleavage during a period of low net primary production (NPP), following a minimum in nitrate concentrations. More generally, we observed an inverse relationship between NPP and $DMSP_d$ cleavage (Type II regression; $r = -0.89$, $p < 0.05$; $n = 6$), suggesting enhanced DMS production associated with lower rates of autotrophic dissolved organic carbon production. Under these conditions, cellular metabolic demands for reduced sulfur are diminished, resulting in greater DMS production relative to DMSP assimilation (Stefels et al. 2007).

Our results suggest that grazing is also an important mechanism for DMS production in the WAP. To date, only a handful of field studies have examined how grazing influences DMS cycling (Kwint et al. 1996; Wolfe et al. 1997, 1999, 2000; Simó et al. 2002; Archer et al. 2003; Salo et al. 2010). These previous studies have shown that grazing can exert a strong control on DMS production in several marine environments, including the Southern Ocean (e.g., Kwint et al. 1996). When the patchy distribution of krill abundance throughout the water column is accounted for, our calculations suggest that microzooplankton generally dominated DMSP release and subsequent DMS production. In addition to the type of grazer, the presence of certain phytoplankton taxa may influence the rates of DMSP removal (release) and subsequent DMS production. For example, we observed a strong negative relationship between the abundance of *Phaeocystis* (single cells) and the removal rate of DMSP (d^{-1}) in micro-grazing experiments (Fig. 4). This result suggests a potential aversion for DMSP-rich and DMSP-lyase containing *Phaeocystis*, and selective feeding by microzooplankton. Conversely, the ratio of DMS produced from $DMSP_t$ increased as a function of *Phaeocystis* abundance ($r = 0.97$, $p < 0.05$; $n = 5$). *Phaeocystis* cells contain compartmentalized cellular DMSP and membrane-bound DMSP-lyase enzyme, which cleaves DMSP to produce DMS (Stefels and Dijkhuizen 1996).

It has previously been assumed that grazing leads to DMS production because sloppy feeding by zooplankton accelerates DMSP cleavage by releasing DMSP from the particulate pool into the dissolved pool in excess of the metabolic requirements or capabilities of bacteria. In this scenario, there is a potential for overlap between our separate measurements of DMS production from micrograzing and $DMSP_d$ cleavage, which could lead to an overestimate in our measurement of overall DMS production. We expect minimal overlap between these measurements for two reasons. Large measurements of DMS production due to grazing coincided with a high abundance of phaeocystis, and thus likely reflected direct DMS production due to the mixing of DMSP-lyase enzyme with DMSP released from cells, not microbial $DMSP_d$ cleavage (Table 4). In addition, tracer experiments were screened for krill and were sampled in a manner not specifically designed to preserve the delicate microzooplankton assemblages.

Results from our grazing experiments suggest that high densities of grazing krill can also lead to DMS production (Dacey and Wakeham 1986) by releasing $DMSP_p$ into the dissolved pool, thereby stimulating DMSP cleavage and slowing gross DMS loss (Fig. 5). Our results provide evidence that excretion of $DMSP_d$ during krill grazing could also contribute to DMSP release. Several studies have shown that zooplankton fecal pellets (e.g., Kwint and Kramer 1996) and zooplankton tissues (Levasseur et al. 1994) contain high concentrations of DMSP, and that the ingestion of plankton by higher trophic level organisms is a mechanism for direct DMS production (e.g., Curson et al. 2009). Krill could excrete DMS as well as DMSP after ingesting DMSP-rich phytoplankton that also contain DMSP lyase. Our krill grazing experiments were all conducted in mid-February when single-celled *Phaeocystis* abundance was highest (Shellie Bench pers. comm.; Fig. 2). Algal intracellular DMSP in the intestines of zooplankton could mix with free DMSP-lyase enzyme to produce DMS in solution, independent of bacterial or algal activity. This mechanism is consistent with the high DMS and DMSP content of juvenile krill and their fecal material (Supporting Information Table S1). We thus conclude that grazing has the potential to accelerate DMS production through direct and indirect pathways, although our experimental protocol does not allow us to explicitly quantify the direct DMS production due to zooplankton excretion.

DMS removal

As part of our field study, we calculated DMS removal due to sea-air flux, and measured rates of gross DMS loss, including biological DMS consumption and photo-oxidation. Compared with gross DMS loss, sea-air flux represented a minor (<10%) sink for DMS until late February, as previously demonstrated by Hermann et al. (2012). Similarly, our results and those of Hermann et al. (2012) indicate that photo-oxidation typically represented a small fraction (<20%) of gross DMS loss at Palmer Station, even in surface waters. Indeed, using the DMS removal relationship between the UV-A light dose and DMS removal due to photolysis observed in Toole et al. (2004), we estimate maximum rates

of surface water DMS photo-oxidation of 2.4 ± 1.5 nM d^{-1}, with a corresponding rate constant of 0.67 ± 0.35 d^{-1}. For this reason, our measured gross DMS loss rates (based on D3 tracer or CI experiments) should largely reflect biological consumption.

It is currently believed that heterotrophs are solely responsible for biological DMS consumption (Vila-Costa et al. 2006b). In support of this, we found that bacterial production was correlated with gross DMS loss (Fig. 6), suggesting that DMS was used (along with DMSP) as a source of bacterial sulfur and energy (Zubkov et al. 2002). Unfortunately, we lack information on the taxonomic composition of the bacterial assemblages and on the contribution of particular clades to the observed DMS metabolism. Based on previous studies, however, we would expect that the presence of particular groups (e.g., *Roseobacter, and Methylophaga*), would be particularly important in determining biological DMS consumption rates (Zubkov et al. 2002; Vila-Costa et al. 2006b).

Neither vertical diffusivity nor lateral advection measurements were part of this study, however, examination of CTD data in early December shows an upwards doming of isohalines in mid-December, indicative of deep-water entrainment or lateral advection (Tortell et al. 2014). Although we lack depth-resolved data on DMS/P/O concentrations throughout the seasonal cycle (we collected samples for only three depth profiles), we presume that sub-surface concentrations would be lower than surface values in early spring, such that dilution could help explain the rapid reduction in DMS concentrations following the DMS maximum in mid-December.

Conclusions and future outlook

This study provides new insight into rapid DMS/P/O cycling in the WAP using a combination of high-resolution DMS/P/O measurements, stable isotope tracer experiments, and grazing assays. Results from this fieldwork show that (1) $DMSP_t$ accumulation is tied to the abundance of *Phaeocystis*, (2) $DMSP_d$ is the main precursor of DMS (3) grazing, particularly by microzooplankton, is a significant source of DMS production, (4) bacterial consumption likely controls DMS removal, and (5) independent factors control $DMSP_d$ cleavage and DMS consumption rate constants.

The Palmer Station LTER site is an important resource for studies of seasonal and inter-annual DMS/P/O variability in the rapidly changing waters of the WAP (Stammerjohn et al. 2008). The Station is located at the northern-most tip of the LTER sampling grid, where significant warming and altered sea-ice dynamics have been observed over the past several decades. Primary production and krill abundance in the northern WAP have declined, and further stratification of the water column has favored the accumulation of diatoms and cryptophytes. New controlling factors in DMS cycling may emerge as phytoplankton bloom dynamics respond to shifts in the timing of sea-ice retreat and stratification (Vernet et al. 2008; Ducklow et al. 2013). Based on the dependence of DMS/P production and concentrations on *Phaeocystis* and grazing, we expect that DMS concentrations at Palmer Station (and in the northern half of the LTER grid) could decline with a further shift towards diatom-dominance. Palmer Station thus provides a unique opportunity to study the effects of climate change on the DMS cycle in polar marine waters.

Looking ahead, more data are needed on the temporal variability in DMS/P/O concentrations and DMS production/consumption terms throughout the seasonal cycle, and our understanding would benefit from an inter-comparison of stable isotope and radioisotope labeled tracer techniques. In addition, more information is needed to constrain the impact of physical processes on DMS/P/O concentrations and turnover rates. In our study, we tracked the mixed layer depth using measurements of temperature and salinity from Stn. B, although we were unable to measure either dynamic vertical mixing or lateral advection. However, previous studies have suggested that dilution can significantly influence phytoplankton bloom dynamics (Tortell et al. 2014; Stukel et al. 2015). Dilution due to vertical mixing or entrainment in our study area may have been particularly important between 01 Dec and 17 Dec (Tortell et al. 2014). Recent upgrades to sampling capabilities at Palmer Station, including the acquisition of a Lidar system to measure surface current flows (O. Schofield pers. comm.), and the potential future deployment of instrumented moorings will provide better insight into the physical processes driving DMS/P/O variability. We believe that continued deployment of automated analytical systems for DMS/P/O concentration measurements, along with advanced process studies, will be an important addition to on-going biogeochemical studies at Palmer Station, and potentially other monitoring sites in polar marine waters. We also note the importance of a regional ocean model for the WAP region including a sulfur-specific biogeochemical module.

References

Archer, S. D., C. E. Stelfox-Widdicombe, P. H. Burkill, and G. Malin. 2001. A dilution approach to quantify the production of dissolved dimethylsulphoniopropionate and dimethyl sulphide due to microzooplankton herbivory. Aquatic Microbial Ecol. **23**: 131–154. doi:10.3354/ame023131

Archer, S. D., C. E. Stelfox-Widdicombe, G. Malin, and P. H. Burkill. 2003. Is dimethyl sulphide production related to microzooplankton herbivory in the southern North Sea? J. Plankton Res. **25**: 235–242. doi:10.1093/plankt/25.2.235

Arrigo, K. R., D. H. Robinson, D. L. Worthen, R. B. Dunbar, G. R. DiTullio, M. VanWoert, and M. P. Lizotte. 1999. Phytoplankton community structure and the drawdown

of nutrients and CO2 in the Southern Ocean. Science. **283**: 365–367. doi:10.1126/science.283.5400.365

Arrigo, K. R., G. R. DiTullio, R. B. Dunbar, D. H. Robinson, M. VanWoert, D. L. Worthen, and M. P. Lizotte. 2000. Phytoplankton taxonomic variability in nutrient utilization and primary production in the Ross Sea. J. Geophys. Res. Oceans. **105**: 8827–8845. doi:10.1029/1998jc000289

Arrigo, K. R., G. van Dijken, and M. Long. 2008. Coastal Southern Ocean: A strong anthropogenic CO2 sink. Geophys. Res. Lett. **35**: doi:10.1029/2008gl035624

Asher, E. C., J. W. H. Dacey, M. M. Mills, K. R. Arrigo, and P. D. Tortell. 2011. High concentrations and turnover rates of DMS, DMSP and DMSO in Antarctic sea ice: DMS dynamics in Antarcic sea ice. Geophys. Res. Lett. **38**: n/a–n/a. doi:10.1029/2011GL049712

Bates, T. S., B. K. Lamb, A. Guenther, J. Dignon, and R. E. Stoiber. 1992. Sulfur emission to the atmosphere from natural sources. J. Atmos. Chem. **14**: 315–337. doi:10.1007/BF00115242

Bernard, K. S., D. K. Steinberg, and O. M. E. Schofield. 2012. Summertime grazing impact of the dominant macrozooplankton off the Western Antarctic Peninsula. Deep Sea Res. Part 1 Oceanogr. Res. Pap. **62**: 111–122. doi:10.1016/j.dsr.2011.12.015

Berresheim, H., J. W. Huey, R. P. Thorn, F. L. Eisele, D. J. Tanner, and A. Jefferson. 1998. Measurements of dimethyl sulfide, dimethyl sulfoxide, dimethyl sulfone, and aerosol ions at Palmer Station, Antarctica. J. Geophys. Res. Atmos. **103**: 1629–1637. doi:10.1029/97jd00695

Boyd, P. W., and others. 2000. A mesoscale phytoplankton bloom in the polar Southern Ocean stimulated by iron fertilization. Nature. **407**: 695–702. doi:10.1038/35037500

Challenger, F., and M. I. Simpson. 1948. 320. Studies on biological methylation. Part XII. A precursor of the dimethyl sulphide evolved by Polysiphonia fastigiata. dimethyl-2-carboxyethylsulphonium hydroxide and its salts. J Chem Soc (Resumed) 1591–1597. doi:10.1039/jr9480001591

Charlson, R. J., J. E. Lovelock, M. O. Andreae, and S. G. Warren. 1987. Oceanic phytoplankton, atmospheric sulfur, cloud albedo and climate. Nature. **326**: 655–661. doi:10.1038/326655a0

Curson, A. R. J., M. J. Sullivan, J. D. Todd, and A. W. B. Johnston. 2009. Identification of genes for dimethyl sulfide production in bacteria in the gut of Atlantic Herring (Clupea harengus). ISME J. **4**: 144–146. doi:10.1038/ismej.2009.93

Dacey, J. W. H., and S. G. Wakeham. 1986. Oceanic dimethylsulfide-production during zooplankton grazing on phytoplankton. Science. **233**: 1314–1316. doi:10.1126/science.233.4770.1314

Dacey, J. W. H., and J. Stefels. 2005. Deuterated tracers for dynamics of the DMS system in marine waters. http://www.aslo.org/meetings/santiago2005/abstracts/1892.htm.

del Valle, D. A., D. J. Kieber, D. A. Toole, J. Bisgrove, and R. P. Kiene. 2009. Dissolved DMSO production via biological and photochemical oxidation of dissolved DMS in the Ross Sea, Antarctica. Deep Sea Res. Part I Oceanogr. Res. Pap. **56**: 166–177. doi:10.1016/j.dsr.2008.09.005

Dickson, D. M. J., and G. O. Kirst. 1987. Osmotic adjustment in marine eukaryotic algae: the role of inorganic ions quarternary ammonium, tertiary sulfphonium and carbohydrate solutes in I. diatoms and rhodophyte. New Phytol. **106**: 645–655. doi:10.1111/j.1469-8137.1987.tb00165.x

DiTullio, G. R., and W. O. Smith. 1995. Relationship between dimethylsulfide and phytoplankton pigment concentrations in the Ross Sea, Antarctica. Deep Sea Res. Part I Oceanogr. Res. Pap. **42**: 873–892. doi: 10.1016/0967-0637(95)00051-7

DiTullio, G. R., and others. 2000. Rapid and early export of Phaeocystis antarctica blooms in the Ross Sea, Antarctica. Nature. **404**: 595–598. doi:10.1038/35007061

Ducklow, H., and others. 2013. West Antarctic Peninsula: an ice-dependent Coastal Marine ecosystem in transition. Oceanography. **26**: 190–203. doi:10.5670/oceanog.2013.62

Everitt, D. A., S. W. Wright, J. K. Volkman, D. P. Thomas, and E. J. Lindstrom. 1990. Phytoplankton community in the Western Equatorial Pacific determined from chlorophyll and carotenoid pigment distributions. Deep Sea Res. Part A Oceanogr. Res. Pap. **37**: 975–997. doi:10.1016/0198-0149(90)90106-6

Fuse, H., O. Takimura, K. Kamimura, K. Murakami, Y. Yamaoka, and Y. Murooka. 1995. Transformation of dimethyl sulfide and related-compounds by cultures and cell-extracts of marine phytoplankton. Biosci. Biotechnol. Biochem. **59**: 1773–1775. doi: 10.1271/bbb.59.1773

Galindo, V., and others. 2015. Under-ice microbial dimethylsulfoniopropionate metabolism during the melt period in the Canadian Arctic Archipelago. Marine Ecol. Progress Series. **524**: 39–53. doi:10.3354/meps11144

Goldman, J. A. L., S. A. Kranz, J. N. Young, P. D. Tortell, R. H. R. Stanley, M. L. Bender, and F. M. M. Morel. 2015. Gross and net production during the spring bloom along the Western Antarctic Peninsula. New Phytologist. **205**: 182–191. doi:10.1111/nph.13125

Gondwe, M., M. Krol, W. Gieskes, W. Klaassen, and H. de Baar. 2003. The contribution of ocean-leaving DMS to the global atmospheric burdens of DMS, MSA, SO2, and NSS SO4=. Global Biogeochemical Cycles. **17**: doi:10.1029/2002gb001937

Hatton, A. D., L. Darroch, and G. Malin. 2005. The role of dimethylsulphoxide in the marine biogeochemical cycle of dimethylsulphide, p. 29–55. *In* Oceanography and marine biology: an Annual Review, Vol. 42.

Herrmann, M., and others. 2012. Diagnostic modeling of dimethylsulfide production in coastal water west of the Antarctic Peninsula. Cont. Shelf Res. **32**: 96–109. doi:10.1016/j.csr.2011.10.017

Jarníková, T., and P. D. Tortell. 2016. Towards a revised climatology of summertime dimethylsulfide concentrations

and sea–air fluxes in the Southern Ocean. Environ. Chem. **13**: 364. doi:10.1071/EN14272

Kieber, D. J., J. F. Jiao, R. P. Kiene, and T. S. Bates. 1996. Impact of dimethylsulfide photochemistry on methyl sulfur cycling in the equatorial Pacific Ocean. J. Geophys. Res. Oceans. **101**: 3715–3722. doi:10.1029/95jc03624

Kiene, R. P., and G. Gerard. 1995. Evaluation of glycine betaine as an inhibitor of dissolved dimethylsulfoniopropionate degradation in coastal waters. Marine Ecol. Progress Series. **128**: 121–131. doi: 10.3354/meps128121

Kiene, R. P., and L. J. Linn. 2000. The fate of dissolved dimethylsulfoniopropionate (DMSP) in seawater: Tracer studies using S-35-DMSP. Geochim. Cosmochim. Acta. **64**: 2797–2810. doi: 10.1016/S0016-7037(00)00399-9

Kiene, R. P., and D. Slezak. 2006. Low dissolved DMSP concentrations in seawater revealed by small-volume gravity filtration and dialysis sampling. Limnol Oceanogr Methods. **4**: 80–95. doi: 10.4319/lom.2006.4.80

Kiene, R. P., D. J. Kieber, D. Slezak, D. A. Toole, D. A. del Valle, J. Bisgrove, J. Brinkley, and A. Rellinger. 2007. Distribution and cycling of dimethylsulfide, dimethylsulfoniopropionate, and dimethylsulfoxide during spring and early summer in the Southern Ocean south of New Zealand. Aquatic Sci. **69**: 305–319. doi:10.1007/s00027-007-0892-3

Kirst, G. O., C. Thiel, H. Wolff, J. Nothnagel, M. Wanzek, and R. Ulmke. 1991. Dimethylsulfoniopropionate (DMSP) in ice-algae and its possible biological role. Marine Chem. **35**: 381–388. doi:10.1016/S0304-4203(09)90030-5

Kwint, R. L. J., and K. J. M. Kramer. 1996. A new sensitive tracer for the determination of zooplankton grazing activity. J. Plankton Res. **18**: 1513–1518. doi:10.1093/plankt/18.8.1513

Lana, A., and others. 2011. An updated climatology of surface dimethlysulfide concentrations and emission fluxes in the global ocean. Global Biogeochem Cycles. **25**: 1–17. doi: Gb1004 10.1029/2010gb003850

Landry, M. R., and R. P. Hassett. 1982. Estimating the grazing impact of marine micro-zooplankton. Marine Biol. **67**: 283–288. doi:10.1007/bf00397668

Landry, M. R., J. Kirshtein, and J. Constantinou. 1995. A refined dilution technique for measuring the community grazing impact of microzooplankton, with experimental tests in the central Equatorial Pacific. Marine Ecol. Progress Series. **120**: 53–63. doi:10.3354/meps120053

Laroche, D., and others. 1999. DMSP synthesis and exudation in phytoplankton: a modeling approach. Marine Ecol. Progress Series. **180**: 37–49. doi: 10.3354/meps180037

Le Clainche, Y., and others. 2006. Modeling analysis of the effect of iron enrichment on dimethyl sulfide dynamics in the NE Pacific (SERIES experiment). J Geophys. Res. **111**: https://core.ac.uk/download/files/387/11700863.pdf. doi:10.1029/2005JC002947

Levasseur, M. 2013. Impact of Arctic meltdown on the microbial cycling of sulphur. Nat. Geosci. **6**: 691–700. doi:10.1038/ngeo1910

Levasseur, M., M. D. Keller, E. Bonneau, D. D'Amours, and W. K. Bellows. 1994. Oceanographic Basis of a DMS-Related Atlantic Cod (*Gadus morhua*) Fishery Problem: Blackberry Feed. Can. J. Fish. Aquat. Sci. **51**: 881–889. doi:10.1139/f94-087

Lovelock, J. E., R. J. Maggs, and R. A. Rasmussen. 1972. Atmospheric dimethyl sulphide and the natural sulphur cycle. Nature. **237**: 452–453. doi:10.1038/237452a0

Luce, M., and others. 2011. Distribution and microbial metabolism of dimethylsulfoniopropionate and dimethylsulfide during the 2007 Arctic ice minimum. J Geophys Res Oceans. **116**: doi:10.1029/2010jc006914

Mahajan, A. S., S. Fadnavis, M. A. Thomas, L. Pozzoli, S. Gupta, S.-J. Royer, A. Saiz-Lopez, and R. Simó. 2015. Quantifying the impacts of an updated global dimethyl sulfide climatology on cloud microphysics and aerosol radiative forcing. J Geophys. Res. Atmos. **120**: 2524–2536. doi: 10.1002/2014JD022687

Merzouk, A., and others. 2006. DMSP and DMS dynamics during a mesoscale iron fertilization experiment in the Northeast Pacific - Part II: biological cycling. Deep Sea Res. Part 2 Top Stud. Oceanogr. **53**: 2370–2383. doi: 10.1016/j.dsr2.2006.05.022

Nightingale, P. D., and others. 2000. In situ evaluation of air-sea gas exchange parameterizations using novel conservative and volatile tracers. Global Biogeochem. Cycles. **14**: 373–387. doi: 10.1029/1999GB900091

Salo, V., R. Simo, and A. Calbet. 2010. Revisiting the dilution technique to quantify the role of microzooplankton in DMS(P) cycling: laboratory and field tests. J. Plankton Res. **32**: 1255–1267. doi:10.1093/plankt/fbq041

Saltzman, E. S., D. B. King, K. Holmen, and C. Leck. 1993. Experimental-determination of the diffusion-coefficient of dimethylsulfide in water. J. Geophys. Res. Oceans. **98**: 16481–16486. doi: 10.1029/93JC01858

Seymour, J. R., R. Simo, T. Ahmed, and R. Stocker. 2010. Chemoattraction to dimethylsulfoniopropionate throughout the marine microbial food web. Science. **329**: 342–345. doi:10.1126/science.1188418

Simon, M., and F. Azam. 1989. Protein content and protein synthesis rates of planktonic marine bacteria. Marine Ecol Progress Series. **51**: 201–213. doi: 10.3354/meps051201

Smith, D. C., and F. Azam. 1992. A simple, economical method for measuring bacterial protein synthesis rates in seawater using 3H- Leucine. Marine Microbial Food Webs. **6**: 107–114.

Spielmeyer, A., B. Gebser, and G. Pohnert. 2011. Investigations of the Uptake of Dimethylsulfoniopropionate by Phytoplankton. ChemBioChem. **12**: 2276–2279. doi: 10.1002/cbic.201100416

Spiese, C. E., D. J. Kieber, C. T. Nomura, and R. P. Kiene. 2009. Reduction of dimethylsulfoxide to dimethylsulfide

by marine phytoplankton. Limnol Oceanogr. **54**: 560–570. doi:10.4319/lo.2009.54.2.0560

Stammerjohn, S. E., D. G. Martinson, R. C. Smith, and R. A. Iannuzzi. 2008. Sea ice in the western Antarctic Peninsula region: Spatio-temporal variability from ecological and climate change perspectives. Deep Sea Res. Part 2 Top Stud. Oceanogr. **55**: 2041–2058. doi:10.1016/j.dsr2.2008.04.026

Stefels, J., and L. Dijkhuizen. 1996. Characteristics of DMSP-lyase in Phaeocystis sp (Prymnesiophyceae). Marine Ecol Progress Series. **131**: 307–313. doi:10.3354/meps131307

Stefels, J., M. Steinke, S. Turner, G. Malin, and S. Belviso. 2007. Environmental constraints on the production and removal of the climatically active gas dimethylsulphide (DMS) and implications for ecosystem modelling. Biogeochemistry. **83**: 245–275. doi:10.1007/s10533-007-9091-5

Stefels, J., J. W. H. Dacey, and J. T. M. Elzenga. 2009. In vivo DMSP-biosynthesis measurements using stable-isotope incorporation and proton-transfer-reaction mass spectrometry (PTR-MS): In vivo DMSP production. Limnol Oceanogr Methods. **7**: 595–611. doi:10.4319/lom.2009.7.595

Stukel, M. R., E. Asher, N. Couto, O. Schofield, S. Strebel, P. Tortell, and H. W. Ducklow. 2015. The imbalance of new and export production in the western Antarctic Peninsula, a potentially "leaky" ecosystem. Global Biogeochem. Cycles. **29**: 1400–1420. doi:10.1002/2015GB005211

Sunda, W., D. J. Kieber, R. P. Kiene, and S. Huntsman. 2002. An antioxidant function for DMSP and DMS in marine algae. Nature. **418**: 317–320. doi: 10.1038/nature00851

Toole, D. A., D. J. Kieber, R. P. Kiene, E. M. White, J. Bisgrove, D. A. del Valle, and D. Slezak. 2004. High dimethylsulfide photolysis rates in nitrate-rich Antarctic waters. Geophys. Res. Lett. **31**: doi:10.1029/2004gl019863

Tortell, P. D. 2005. Dissolved gas measurements in oceanic waters made by membrane inlet mass spectrometry. Limnol. Oceanogr. Methods. **3**: 24–37. doi:10.4319/lom.2005.3.24

Tortell, P. D., and M. C. Long. 2009. Spatial and temporal variability of biogenic gases during the Southern Ocean spring bloom. Geophys. Res. Lett. **36**: doi:L01603 10.1029/2008gl035819

Tortell, P. D., C. Gueguen, M. C. Long, C. D. Payne, P. Lee, and G. R. DiTullio. 2011. Spatial variability and temporal dynamics of surface water pCO(2), Delta O-2/Ar and dimethylsulfide in the Ross Sea, Antarctica. Deep Sea Res. Part I Oceanogr. Res. Pap. **58**: 241–259. doi:10.1016/j.dsr.2010.12.006

Tortell, P. D., M. C. Long, C. D. Payne, A. C. Alderkamp, P. Dutrieux, and K. R. Arrigo. 2012. Spatial distribution of pCO_2, $\Delta O_2/Ar$ and dimethylsulfide (DMS) in polynya waters and the sea ice zone of the Amundsen Sea, Antarctica. Deep Sea Res. Part II Top. Stud. Oceanogr. **71–76**: 77–93. doi:10.1016/j.dsr2.2012.03.010

Tortell, P. D., and others. 2014. Metabolic balance of coastal Antarctic waters revealed by autonomous $p\ CO_2$ and $\Delta O_2/Ar$ measurements: metabolic balance of Antarctic waters. Geophys. Res. Lett. **41**: 6803–6810. doi:10.1002/2014GL061266

Vallina, S. M., and R. Simo. 2007. Strong relationship between DMS and the solar radiation dose over the global surface ocean. Science. **315**: 506–508. doi:10.1126/science.1133680

Vernet, M., D. Martinson, R. Iannuzzi, S. Stammerjohn, W. Kozlowski, K. Sines, R. Smith, and I. Garibotti. 2008. Primary production within the sea-ice zone west of the Antarctic Peninsula: I-Sea ice, summer mixed layer, and irradiance. Deep Sea Res. Part II Top Stud Oceanogr. **55**: 2068–2085. doi: 10.1016/j.dsr2.2008.05.021

Vila-Costa, M., R. Simo, H. Harada, J. M. Gasol, D. Slezak, and R. P. Kiene. 2006a. Dimethylsulfoniopropionate uptake by marine phytoplankton. Science. **314**: 652–654. doi:10.1126/science.1131043

Vila-Costa, M., D. A. del Valle, J. M. Gonzalez, D. Slezak, R. P. Kiene, O. Sanchez, and R. Simo. 2006b. Phylogenetic identification and metabolism of marine dimethylsulfide-consuming bacteria. Environ. Microbiol. **8**: 2189–2200. doi:10.1111/j.1462-2920.2006.01102.x

Vila-Costa, M., R. P. Kiene, and R. Simo. 2008. Seasonal variability of the dynamics of dimethylated sulfur compounds in a coastal northwest Mediterranean site. Limnol Oceanogr. **53**: 198–211. doi:10.4319/lo.2008.53.1.0198

Welschmeyer, N. A. 1994. Fluorometric analysis of chlorophyll-a in the presence of chlorophyll b and pheopigments. Limnol. Oceanogr. **39**: 1985–1992. doi:10.4319/lo.1994.39.8.1985

Wingenter, O. W., K. B. Haase, P. Strutton, G. Friederich, S. Meinardi, D. R. Blake, and F. S. Rowland. 2004. Changing concentrations of CO, CH_4, C_5H_8, CH_3Br, CH_3I, and dimethyl sulfide during the southern ocean iron enrichment experiments. Proceed. Nat. Acad. Sci. USA. **101**: 8537–8541. doi:10.1073/pnas.0402744101

Wolfe, G. V., M. Steinke, and G. O. Kirst. 1997. Grazing-activated chemical defence in a unicellular marine alga. Nature. **387**: 894–897. doi:10.1038/43168

Wolfe, G. V., M. Levasseur, G. Cantin, and S. Michaud. 1999. Microbial consumption and production of dimethyl sulfide (DMS) in the Labrador Sea. Aquatic Microbial Ecol. **18**: 197–205. doi:10.3354/ame018197

Wolfe, G. V., M. Levasseur, G. Cantin, and S. Michaud. 2000. DMSP and DMS dynamics and microzooplankton grazing in the Labrador Sea: application of the dilution technique. Deep Sea Res. Part I Oceanogr. Res. Pap. **47**: 2243–2264. doi:10.1016/S0967-0637(00)00028-5

Yang, M., S. D. Archer, B. W. Blomquist, D. T. Ho, V. P. Lance, and R. J. Torres. 2013. Lagrangian evolution of DMS during the Southern Ocean gas exchange experiment: the effects of vertical mixing and biological community shift. J. Geophys. Res. Oceans. **118**: 6774–6790. doi:10.1002/2013jc009329

Zubkov, M. V., B. M. Fuchs, S. D. Archer, R. P. Kiene, R. Amann, and P. H. Burkill. 2002. Rapid turnover of dissolved DMS and DMSP by defined bacterioplankton communities in the stratified euphotic zone of the North Sea.

Deep Sea Res. Part II Top. Stud. Oceanogr. **49**: 3017–3038. doi:10.1016/S0967-0645(02)00069-3

Acknowledgments

We would like to acknowledge the scientific and support staff at Palmer Station, Antarctica for invaluable assistance throughout our field season. In particular, we would like to thank Kim Bernard for contribution of krill biomass data, and her help in designing and conducting these experiments. In addition, we would like to acknowledge Shelly Bench, Johanna Goldman, Sven Kranz, Jodi Young, Nicole Couto and Stephanie Strebel for assistance with zodiac sampling and for providing ancillary data. This work was funded by the US National Science Foundation (OPP awards ANT-0823101, ANT-1043532) as from the National Science and Engineering Research Council of Canada.

Conflict of Interest

None declared.

Submitted 09 July 2015
Revised 23 April 2016
Accepted 27 June 2016

Associate editor: M. Dileep Kumar